Thermal Degradation of Polystyrene

Thermal Degradation of Polystyrene

by

P. De Somer, B. E.

A Project Report

Submitted to the School of Graduate Studies

in Partial Fulfilment of the Requirements

for the Degree

Master of Engineering

McMaster University

September 1973

ACKNOWLEDGEMENTS

The author gratefully acknowledges the guidance and encouragement from Dr. A. E. Hamielec throughout the length of this work. Financial assistance in the form of a McMaster University Scholarship is gratefully appreciated. He also wishes to express his thanks to his fellow graduate student, John Richmond, for his helpful advice.

Master of Engineering (1973) McMaster University
(Chemical Engineering) Hamilton, Ontario

TITLE: Thermal Degradation of Polystyrene

AUTHOR: P. De Somer, B.E. Chem. Eng. (Louvain University, Belgium)

SUPERVISOR: Professor A. E. Hamielec

NUMBER OF PAGES: 81, V

SCOPE AND CONTENTS:

In this study uninhibited styrene, degassed under high vacuum (10^{-6} mm Hg), was thermally polymerized in bulk of 10^{-6} mm Hg up to almost complete conversion. The samples so obtained were thermally degraded under the same high vacuum conditions at temperatures ranging between 270°C and 340°C for different time intervals over the whole range of degradation. The breakdown of the polymer, through changes in number, weight average molecular weights, polydispersity and molecular weight distribution, was investigated using gel permeation chromatography. A mechanism of degradation was sought, and the breakdown explained by a combined process of depolymerization and chain scission. Scission constants were determined and compared with the constants, obtained from a polystyrene having much larger molecular weights.

TABLE OF CONTENTS

A P P E N D I X

1. Calculation of the total number of polymer particles from the GPC response

2. Second method for calculating the chain length dependence of the depropagation constant in model 2

3. Tables

   1. Properties of the undegraded polymer samples
   2. k_{dp} $(\bar{n})$ at different temperatures.
   3. Degradation of polymer I at 270°C
   4. Degradation of polymer I at 292°C
   5. Degradation of polymer I at 311°C
   6. Degradation of polymer I at 336°C
   7. Degradation of polymer II at 311°C

I INTRODUCTION

During the last few decades the effect of high temperatures on the stability of natural and synthetic polymers has been investigated extensively.

Studies on the thermal behavior of polymers, particularly on their thermal degradation, are of primary importance from a scientific point of view [1]. Such studies help to reveal the molecular structure, such as the sequence and arrangement of the repeating units, or monomers, and side groups in the polymer or copolymer chain. Such studies also throw light on the strength of the various bonds holding together the repeat units of polymer molecules, on the kinetics of depolymerization, on the effects of time, temperature, pressure and other variables, on rates and products of degradation. Similarly, studies on the thermal degradation of polymers are of extreme importance from a practical point of view. They not only explain the behaviour of polymers at high temperatures, but also help in selecting the right kind of already existing materials for specific uses where high temperatures are encountered, e.g. in the processes of pressure molding, extrusion and casting, and, what is sometimes even more important, suggest the design and synthesis of new materials to meet new or existing requirements.

In the classical chemical sense, the term degradation means breaking down of structure or reduction of molecular weight [15]. There are two general types of polymer degradation processes, corresponding

roughly to the two types of polymerization, step-reaction and chain reaction:

(*) Random Degradation: is analogous to stepwise polymerization. Here chain rupture or scission occurs at random points along the chain, leaving fragments which are usually large compared to a monomer unit.

(**) Chain Depolymerization: involves the successive release of monomer units from a chain end in a depropagation or unzipping reaction which is essentially the reverse of chain polymerization.

These two types may occur separately or in combination, being initiated thermally they may occur entirely at random or preferentially at chain ends or at other weak links in the chain. It is possible to differentiate between the two processes in some cases by following the molecular weight of the residue as a function of the extent of degradation. Molecular weight drops rapidly as random degradation proceeds but may remain constant in chain depolymerization (fast unzipping), as whole molecules are reduced to monomer, which escapes from the residual sample as a gas. This is one of the criteria on which we will analyze our data. The degradation products are also different for the two processes: the ultimate product of random degradation is likely to be a disperse mixture of molecular weight up to several hundred, whereas chain depolymerization yields large quantities of monomer. For polystyrene the degradation products were extensively analyzed (2,3).

A great deal of the literature on the thermal degradation of polystyrene refers to work done in a vacuum. The main reason for this lies in the fact that when the polymers are heated in a gaseous atmosphere, even if it is neutral, the diffusion out of the sample of volatile prod-

ucts which are formed inside it is retarded so that these products may undergo secondary reactions. If, instead of in a neutral gas, pyrolysis is carried out in air, there is an additional difficulty arising from the fact that the purely thermal effects of degradation of the polymer will be masked by the chemical reaction of the degradation products, volatile and non-volatile, with oxygen. In studies where it is desired to determine the effect of an external gas or of an oxidizing atmosphere on thermal degradation of polymers, the purely thermal effect can then be subtracted from the overall effects thus obtained.

In the present study the thermal degradation of polystyrene, free of oxygen, was investigated between 270°C and 340°C. Gel permeation chromatography was used as an analytical tool in the study of the thermal degradation. A lot of additional detailed information was thus obtained, giving a clearer picture of the degradation of chains of different molecular weight.

II LITERATURE REVIEW

It is an established fact that the end products of the thermal degradation of polystyrene are 43% volatile materials (this fraction was found by mass spectrometry to be 41% styrene and, with rising temperatures of degradation, progressively decreasing amounts of dimer, trimer, tetramer and pentamer) and 57% residue, which is a low molecular weight fraction [1,2]. These can be qualitatively accounted for in terms of the radical mechanism for depolymerization by depropagation and by intramolecular transfer at chain ends, respectively.

However, a rapid initial decrease in molecular weight is observed as opposed to the linear decrease in molecular weight in the later stages of the reaction. Jellinek [3] and Grassie [4] contend that the initial fall in molecular weight is due solely to scission of "weak" bonds and that in the later stages of the reaction the slower decrease in molecular weight is due to depolymerization in a free radical chain reaction. Jellinek [3] attributed these weak links to oxygen incorporated during polymerization in the polymer chain in the form of peroxide groups. Grassie and Kerr [4] measured the concentration of such weak links from the extent of the initial decrease in molecular weight. Cameron and Grassie [5] have attributed these weak links to structures of the type

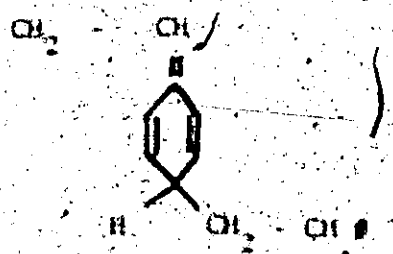

On the other hand Madorsky [6] and Wall [7] and coworkers assert that there is no essential difference between the initial and final stages of the reaction, and that the changes in molecular weight are due predominantly to intermolecular chain transfer reactions, following a chain-end initiation step which produces the primary radicals.

More recently Richards and Salter [8] have suggested that both processes, weak link scission and intermolecular chain transfer, are involved in the reaction.

Both interpretations of the reaction are open to criticism. Grassie's method [4] of estimating weak bond concentration is insensitive and in certain circumstances could be misleading. Simha's and Wall's conclusions [7] are based upon a comparison of experimental results and a sophisticated theoretical treatment. The correspondence between theory and experiment, however, is not convincingly exact for a wide range of initial molecular weights or at low conversions.

Difficulties of interpretation arise because of the complicating effects of volatile formation on the chain scission reactions. An attempt by Cameron and Kerr [9] was made to overcome this by studying the thermal degradation of thermally and anionically prepared polystyrenes at temperatures where volatile formation was assumed to be negligible (280 - 300°C). Plots of the degree of degradation, α*, versus time are linear, confirming the random nature of the chain scission reactions.

---

*Degree of degradation α is defined as $\frac{1}{(DP)_t} - \frac{1}{(DP)_0}$,

where DP = degree of polymerization

The lines for anionic polymers pass within experimental error through the origin, but these for the thermally polymerized samples all show a substantial intercept on the α-axis at zero time. This behaviour is interpreted as associated with "weak" links in the polymer chains. The number of weak links, calculated from the size of the intercept of the α versus time plot, is independent of the temperature of degradation and was about 5.15×10^{-5} scissions per chain link. These weak links might be distributed at random within the polymerchains and might be formed by a copolymerized impurity or by an abnormal propagation step during the polymerization. These groups would break down very early in the reaction.

It should be stated clearly that up to now all the modeling done on the thermal degradation of polystyrene has been qualitative. Attempts were made to model the experimental data [7, 22], the results however are unconvincing.

One limitation of the earlier studies on the thermal degradation of polystyrene, stems from the inherent assumption of a constant molecular weight distribution, of the latter investigations that at temperatures between 280°C and 310°C devolatilization is negligible. Our results show that this is not so. With increasing degradation time the dispersity of the polymer decreases and more volatile products are formed. Also up to now all the work on thermal degradation was done using dynamic thermogravimetric analysis [10], never before gel permeation chromatography was used as an experimental tool, although, as will become clear from this work, a lot of additional information can be obtained, mainly on the behaviour of the chains individually. Further degassing

of the styrene monomer at 10^{-6} mm Hg, and carrying out polymerization and consecutive degradation under the same high vacuum conditions, should almost rule out the existence of Jellinek's weak bonds, due to peroxide groups.

III EXPERIMENTAL CONDITIONS

III-1 General Conditions

Inhibited styrene was obtained from Monsanto, Montreal, Canada. The inhibitor was removed using a sodium hydroxide solution. After distillation the refractive index of the monomer was tested using an Abbe-refractometer. The refractive index at 21°C was found to be the same as in the literature [11]: $n_{D,\ 21^{\circ}C} = 1{,}5469$ (vs 1.5482 for inhibited styrene). This inhibited styrene, used for all polymerization reactions without further purification, was stored in a refrigerator until use. All polymerization reactions and degradation experiments were carried out in sealed Pyrex glass ampoules [12]. The size was of standard Pyrex glass tubing of 9 mm O.D. corresponding to 7 mm I.D. The geometry of these ampoules is shown in Figure III-1. A steady state heat conduction balance proved the temperature difference between wall and center of the tube to be negligible (~ 0.36°C) as reported by Hui [12].

Extreme care was taken on the degassing of the monomer. The reactant, consisting of styrene monomer, was prepared and introduced into the glass ampoules. They were sealed, after being degassed under vacuum to the order of 10^{-6} mm Hg pressure. These sealed ampoules were then used for polymerization and subsequent degradation.

The vacuum line required for the degassing operation was a standard high vacuum apparatus. It consisted of a rotary backing pump, a mercury diffusion pump, a McLeod gauge, a cold trap and ten valved standard taper joints. The schematic diagram is shown in Figure III-2. The com-

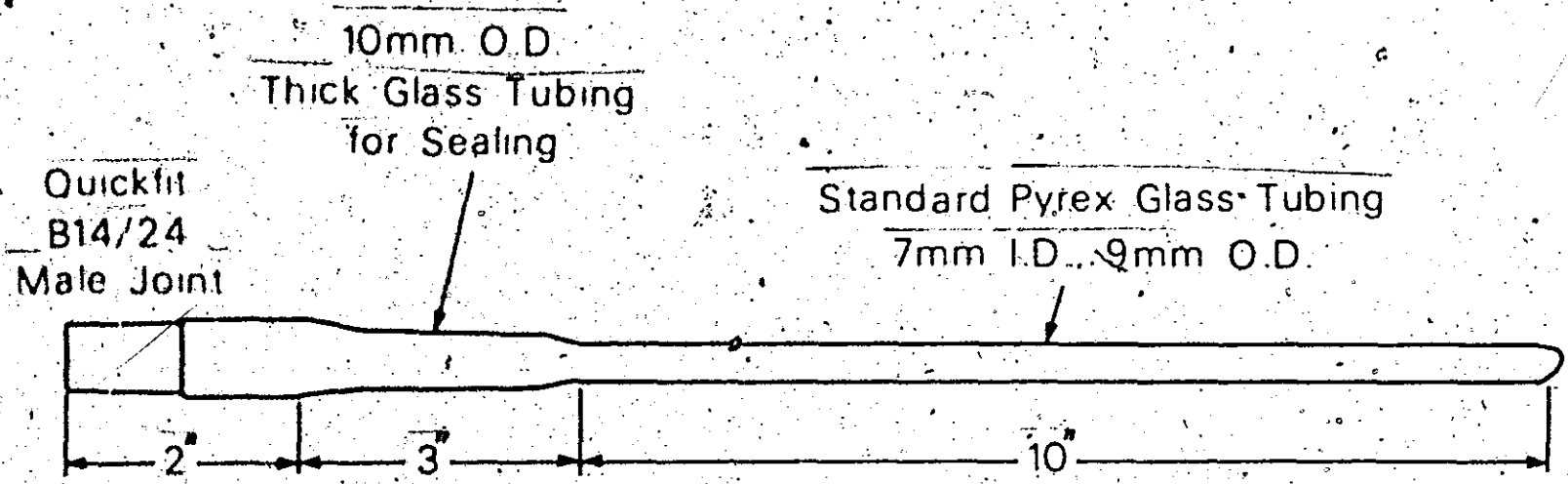

FIG. 1 DIMENSIONS OF GLASS REACTION AMPOULES

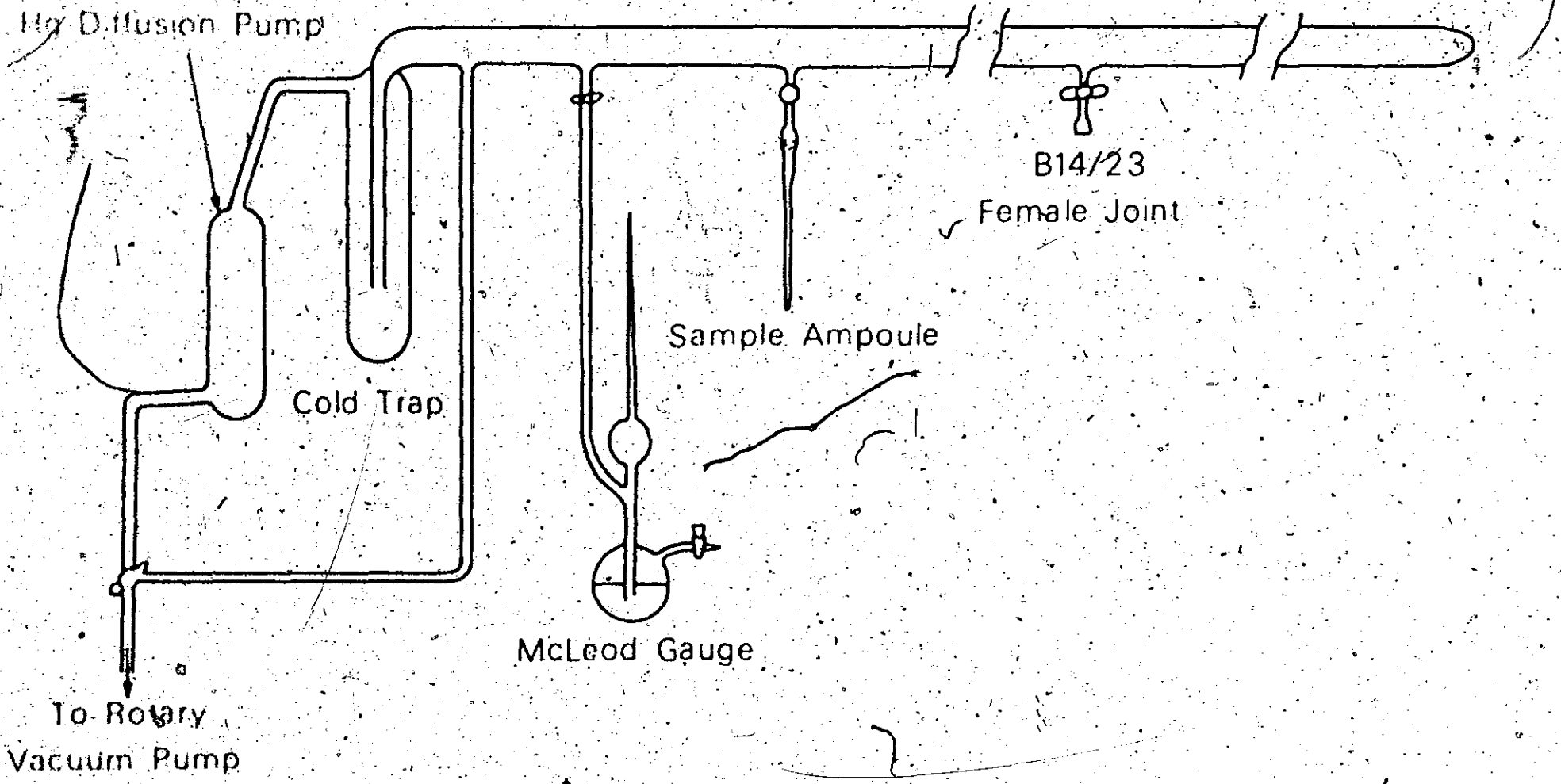

FIG. II-2 SCHEMATIC DIAGRAM OF VACUUM SYSTEM

plete degassing procedure is as follows:

(1) The filled reaction ampoule was connected to the vacuum line, and immersed in liquid nitrogen.

(2) Fifteen minutes later, the valve connecting the ampoule to the vacuum line was open and the reactant ampoule was evacuated for 15 minutes.

(3) The valve was then closed, liquid nitrogen removed, allowing the frozen sample to warm up to room temperature during which the dissolved gasses escaped from the reactant. Cracking of the glass ampoule due to expansion of reactant was prevented by warming the frozen ampoule quickly with warm water after the removal of the surrounding liquid nitrogen.

(4) The flask of liquid nitrogen was put back again to freeze the sample ampoule.

(5) The valve to the vacuum line was opened again and the ampoule evacuated for 15 minutes.

(6) The pressure of the system was tested with the McLeod gauge making sure that an absolute pressure of the order of 10^{-6} mm Hg was obtained.

(7) Liquid nitrogen was removed and the ampoule sealed off using a gas-oxygen torch.

(8) The sealed ampoule was warmed with warm water and put immediately in the oven for poly-

merization.

Both polymerization and degradation were carried out in a Blue M Electric Company Mechanical Convection Oven with a temperature range up to 1000°C. With a built-in proportioning control system a fixed oven temperature (± 1°C) could be obtained. All polymerizations, unless otherwise stated, were carried out at 168°C for 40 hours. The characteristics of the so obtained polymer are given in table 1 in appendix 3 (polymer I). This polymer was subsequently degraded at 270, 292, 311 and 336°C for different time intervals up to almost complete conversion of polymer. This temperature range was chosen for the following reasons: below 270°C the degradation is too slow and consequently too time consuming; above 270°C the degradation is much faster and gives no difficulties in comparison, up to 340°C.

Since at these degradation temperatures a lot of volatile materials are formed the pressure in the system can be expected to rise with increasing amount of these materials being formed. Assuming volatile styrene to be an ideal gas and the only volatile product formed, we calculated that from 6% degradation on (6% of the original polymer degraded) a constant pressure corresponding to the vapour pressure of styrene [14] at the corresponding temperature, was obtained, e.g. 8.9×10^{3} mm Hg at 292°C. Since this constant pressure is obtained so early in the degradation, the whole reaction was assumed to take place under constant pressure.

III-2 Gel Permeation Chromatography

The extent of degradation, number, weight average molecular weight, polydispersity and molecular weight distribution of the de-

graded samples were analyzed using a Waters Model - 200 gel permeation chromatograph. The solvent flowrate was 3.5 mls/min., the concentration of injected samples 0.25 wt. %. The columns used were 2 x CPG 10 - 2,000 Å, 1 x CPG 10 - 700 Å, 1 x CPG 10 - 370 Å, 1 xCPG 10 -240 Å and 2 x CPG 10 - 125 Å. The extent of degradation was determined using monomer and polymer peak integration of the GPC recorder trace. Due to the poor resolution at the lower molecular weight tail the monomer peak probably contains a large amount of di-, tri, ... pentamer. This could also be observed from a small shift to the right of this peak. As in the literature, we will call this then the "volatile"-fraction, since these oligomers are volatile at the degradation temperatures.

Number and weight average molecular weights were corrected for imperfect resolution and axial dispersion using a linear effective calibration curve [13].

Since during the thermal degradation of polystyrene a lot of low molecular weight products are being formed, it would be interesting to investigate the GPC response of these low molecular weights.

In a recent paper [16] Margerison et al. studied the variation of the refractive index with molecular weight, using solutions of monodisperse polystyrenes in toluene. They found that the refractive index difference Δn between the solution and the solvent is not only a function of concentration but also of molecular weight. Their results show an asymptotic approach of the refractive index increment towards a limiting value characteristic of the infinite molecular weight polymer. They find that this limiting value is reached within experimental error in the molecular weight range between 50,000 and 100,000.

This change of refractive index with molecular weight is an important experimental parameter in the treatment of data obtained from GPC. In order to standardize the GPC response for different chain lengths, a correction can be introduced as follows:

$$c(v) = F(v) / \alpha(v)$$

where $c(v)$ = mass/unit volume

$F(v)$ = G.P.C. response height at elution count v

$\alpha(v)$ = proportionality factor depending on elution count or molecular weight.

The normalized heights are then:

$$C_N(v) = \frac{c(v)}{\int c(v)\, dv}$$

$$\text{or } C_N(v) = \frac{F(v)/\alpha(v)}{\int F(v)\, dv/\alpha(v)}$$

In order to investigate the relative importance of these proportionality factors, solutions of 0.1 and 0.2 wt. % polystyrene and molecular weights up to 100,000 were injected. The areas under the GPC response curves were calculated using Simpson's integration rule. The polystyrene samples used were sharp molecular weight fractions obtained from Pressure Chemical Co. The results are shown in table III-1 and figure III-2.

Table III-1

weight fraction (%)	molecular weight	area (x 10^{-4})
0.2	97,200	.93754
	97,200	.89802
	50,000	.92458
	19,750	.87509
	4,800	.88553
	4,800	.90879
	2,030	.85349
	2,030	.87662
	600	.82021
	600	.81439
	Monomer	.79138
	Monomer	.76179
0.1	97,200	.46530
	97,200	.44262
	50,000	.47906
	19,750	.45341
	4,800	.45546
	4,800	.45802
	2,030	.44797
	600	.39750
	Monomer	.36250
	Monomer	.36800

FIG. III-3

AREA UNDER G.P.C. RESPONSE CURVE VS. CONCENTRATION OF SAMPLES INJECTED

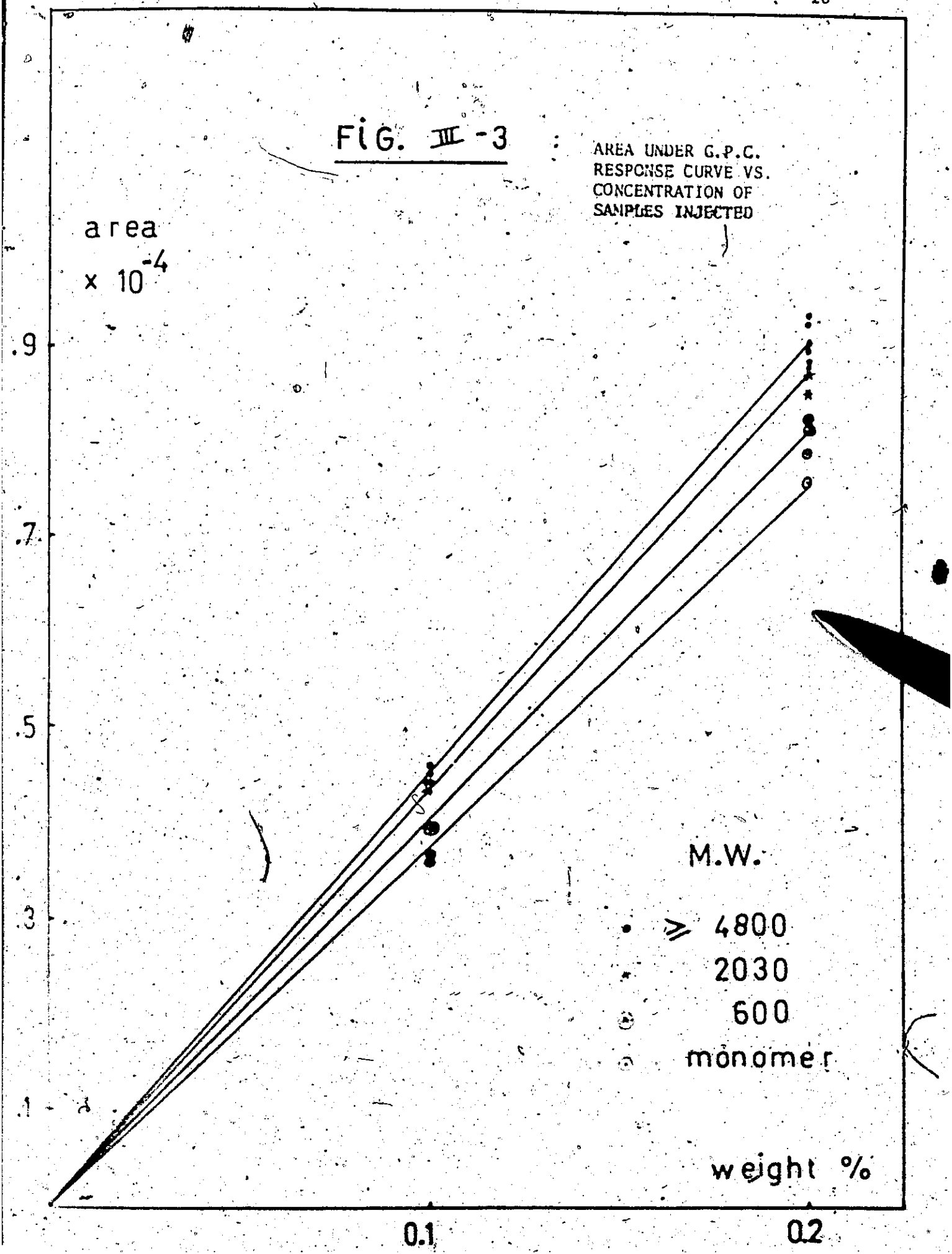

It is clear that in the range of polymer concentrations employed, the refractive index difference, given by the area under the GPC response curve, can be expressed as

$$\Delta\mu = V_m \times w$$

where V_m is the refractive index increment corresponding to the polymer concentrations, being expressed in terms of mass fraction, w, and can be obtained as the slope of the area versus w-curves in figure III-3. The following V_m were obtained:

M.W.	$V_m \times 10$
monomer	.376
600	.408
2,030	.438
4,800 & higher	.455

From a plot of V_m versus molecular weight, figure III-4, it is apparent that, as the polymer molecular weight increases, V_m increases towards a limiting value characteristic of the infinite molecular weight polymer. The point at which the systematic variation of V_m with molecular weight is rendered undetectable by the presence of random errors of measurement depends on the magnitude of these errors. With the GPC technique of data analysis we conclude that V_m effectively reaches its limiting value at a molecular weight somewhere around 5,000, the value V_m being $.455 \times 10^{-1}$.

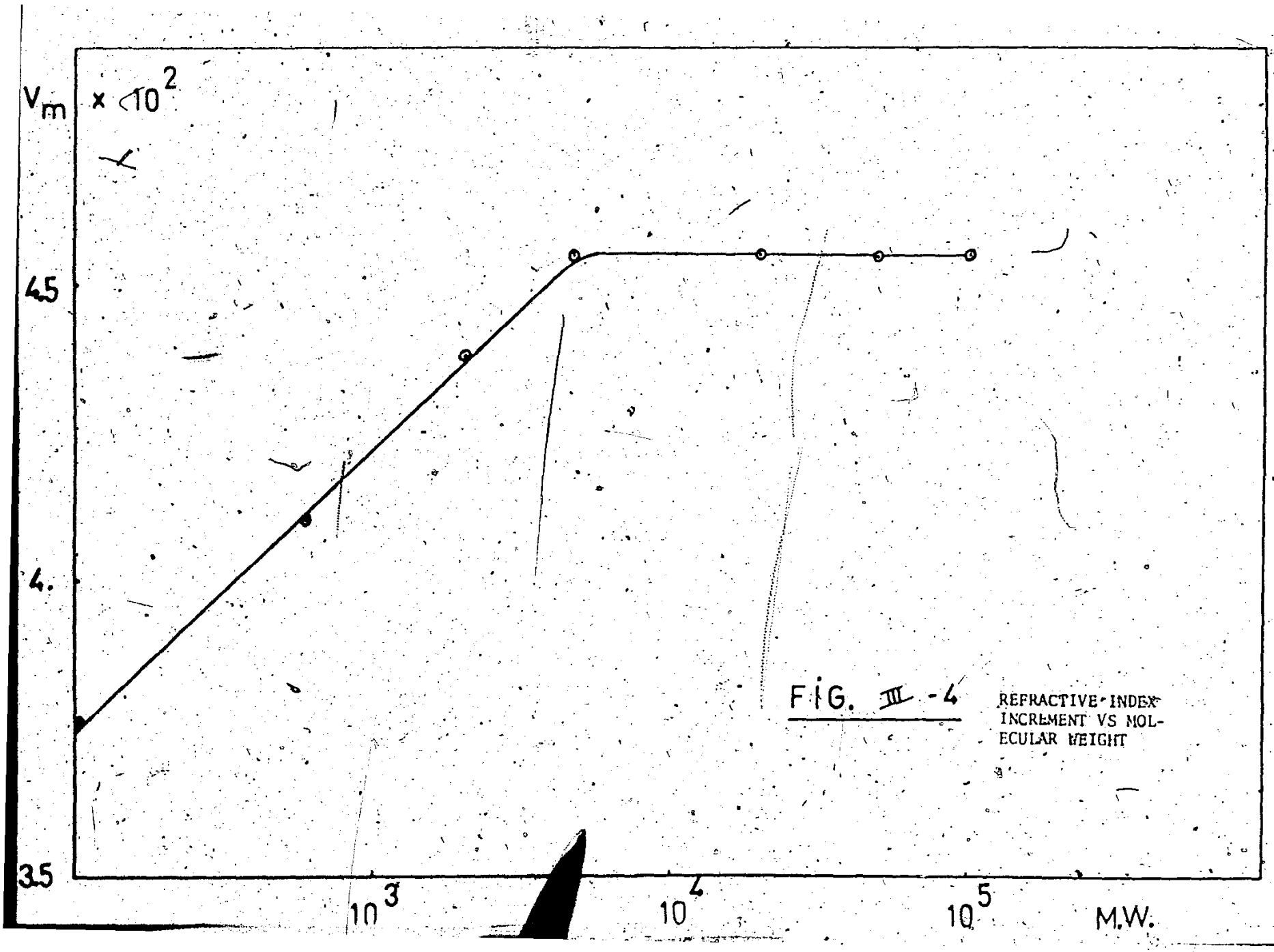

FIG. III -4 REFRACTIVE INDEX INCREMENT VS MOLECULAR WEIGHT

These results can be explained as follows. It is permissible to regard the specific refraction of a polymer solution as being the weighted sum of the specific refractions of the solvent, repeat units and end groups, the latter in our case C_4H_9. The influence of molecular weight on V_m is entirely an end group effect. As the proportion of repeat units to end groups increases, the refractive index increment V_m approaches its limiting value.

The GPC calibration curve is given in figure III-5. As one can see the resolution for the used set of columns at the lower molecular weight tail (< 5,000) is rather poor. This is rather disappointing in view of the large quantities of low molecular weight material formed during thermal degradation. Due to this poorer resolution the corrections at the lower molecular weights become meaningless and were therefore omitted. Although not too much can be said about the lower end of the molecular weight distribution, however the changes in concentration at the intermediate and high molecular weight chains can be clearly seen. It is mainly in these chains that we are interested as they significantly influence the mechanical properties of the polymer and their degradation is certain to seriously reduce the effectiveness of the polymer in many of its applications.

FIG. III - 5

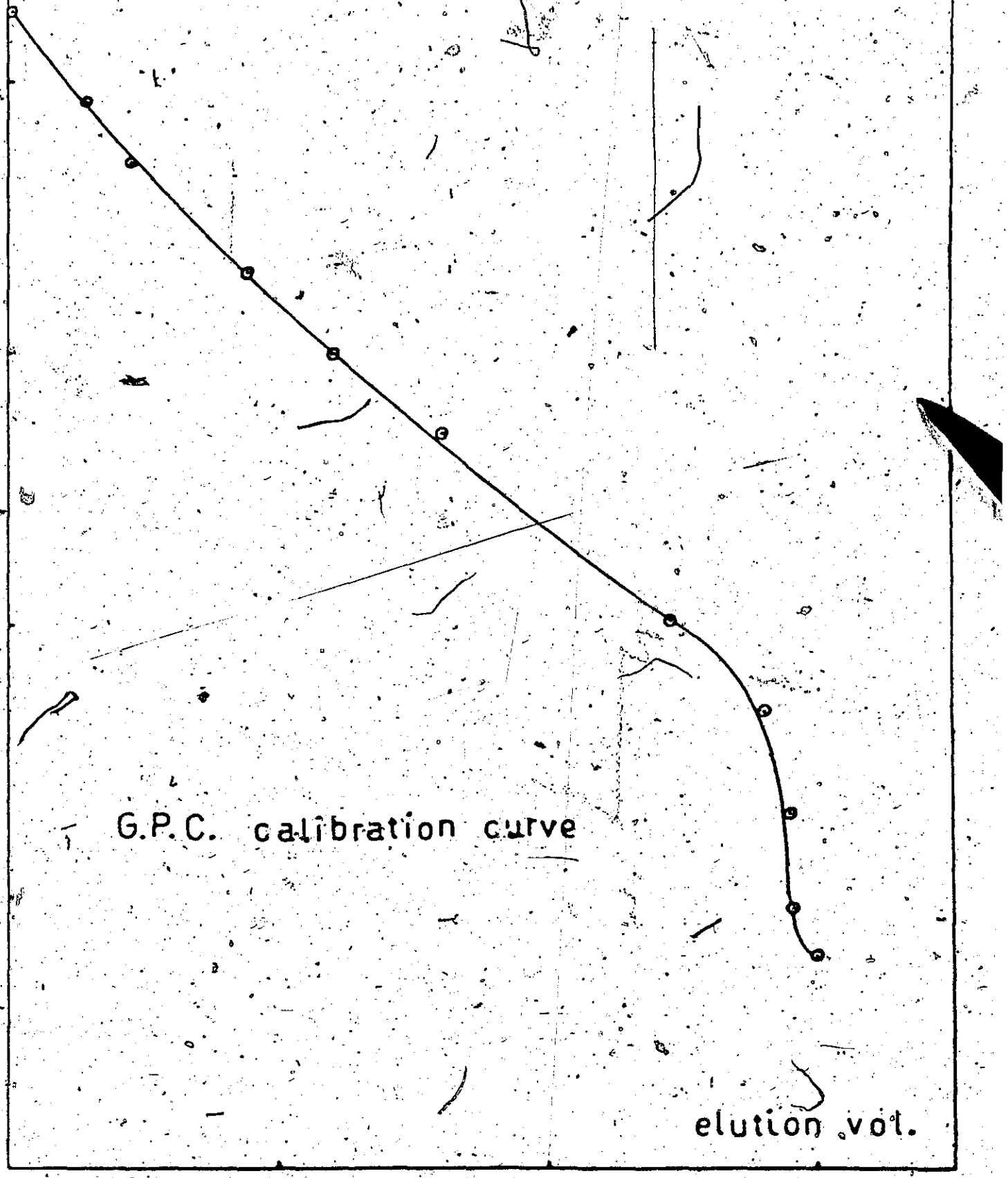

G.P.C. calibration curve

IV EXPERIMENTAL RESULTS AND DISCUSSION

IV-1 Introduction

Since we would like to show in this study how our kinetic model, explaining the thermal degradation of polystyrene, was developed, we will treat experimental results and corresponding discussion simultaneously. This will allow the reader to follow the trend of our ideas, as gradually more experimental data became available.

When we go back to the literature, the initial steep decrease in molecular weight during thermal degradation of polystyrene, is explained by different authors (see literature review) as due to the presence of weak links in the polymerchain. Jellinek [3] specified these weak bonds as peroxide groups, formed in the chain during polymerization.

The idea on which this work was started then was to eliminate these peroxide groups by degassing the styrene monomer and carrying out the subsequent polymerization and degradation at 10^{-6} mm Hg, in order to make sure that no oxygen could interfere with the different processes. This should allow us to make a more stable polymer, where scission of the chains by oxygen could almost be ruled out, and the degradation process described solely through depolymerization (unzipping) of monomer units at the chain ends. Further in the investigation it became clear that this simple "unzipping" model was not adequate to explain the degradation rates. Other mechanisms were analyzed. The different steps were

(a) Unzipping or depolymerization: instantaneous and slow.

(b) Depolymerization with k_{dp} (depropagation constant) function of chain length.

(c) Random scission and depolymerization.

(d) Random scission with k_s (scission constant) function of chain length.

(e) Test of model (d).

As already stated before steps (a), (b), (c), (d) were investigated on styrene polymerized at 168°C under 10^{-6} mm Hg vacuum. The so obtained samples were degraded at the same oxygen level at 270, 292, 311 and 336°C. This gave us a quite broad temperature range and allowed the construction of an Arrhenius plot for the reaction constants.

NOTE: All the data on the different figures can be found back in table form in appendix 3.

IV-2 Model 1: Unzipping or Depolymerization

The first experimental information which became available was the production of monomer or more precisely "volatile" fraction versus time, figure IV-1. To test the poor resolution of the GPC columns at lower molecular weights we also plotted for the different degradation temperatures, the decrease in polymer mass vs time, figure IV-2, and the decrease in polymer larger than molecular weight 20,000 vs time, figure IV-3. All the curves obtained have the same shape: straight lines for the lower temperatures (270°C, 292°C), and partially straight with curvature around 50% volatile fraction for the higher temperatures

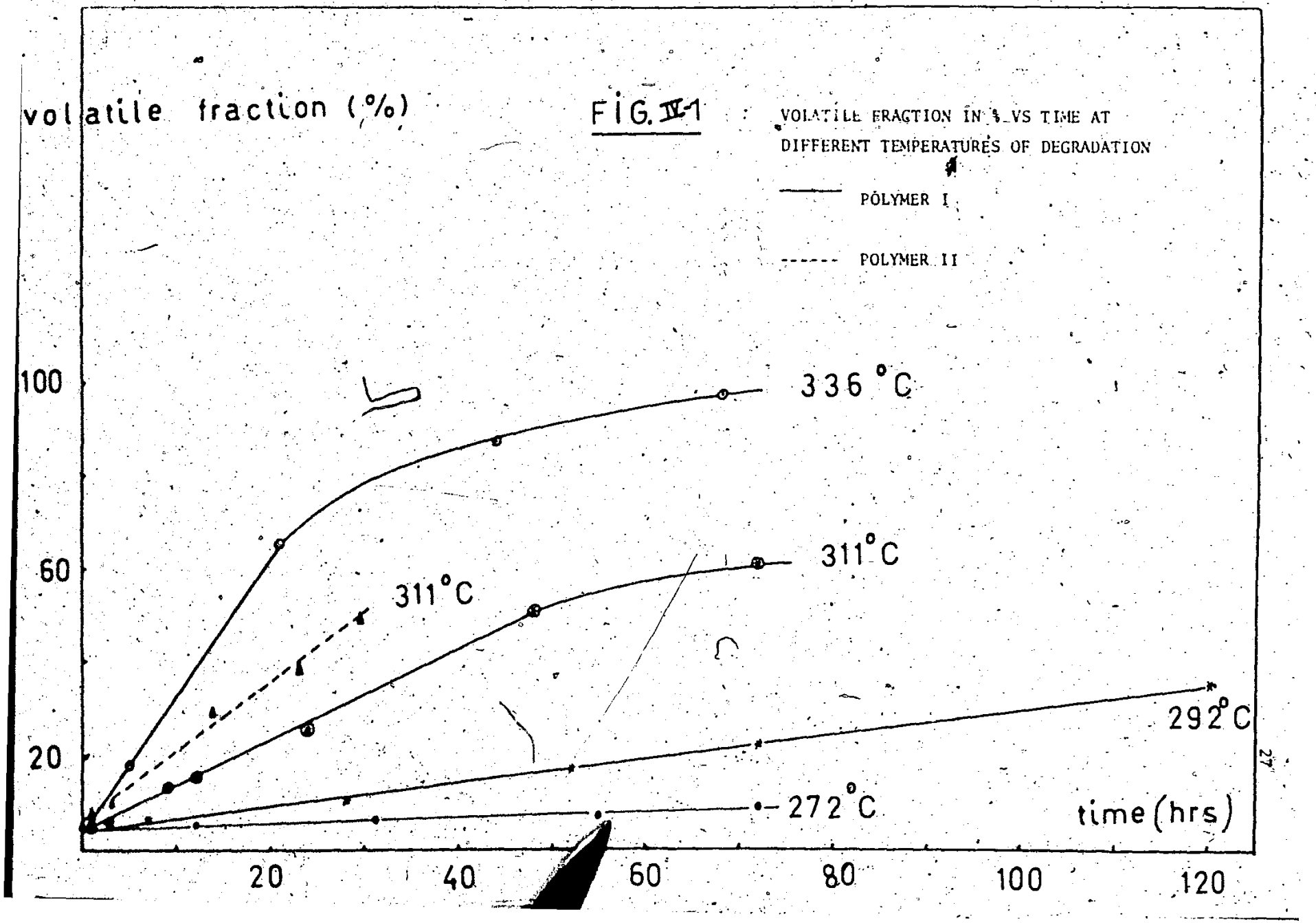
volatile fraction (%)
FIG. IV-1 : VOLATILE FRACTION IN % VS TIME AT DIFFERENT TEMPERATURES OF DEGRADATION
POLYMER I
POLYMER II
100
60
20
336 °C
311°C
311°C
292°C
272°C
time (hrs)
20
40
60
80
100
120

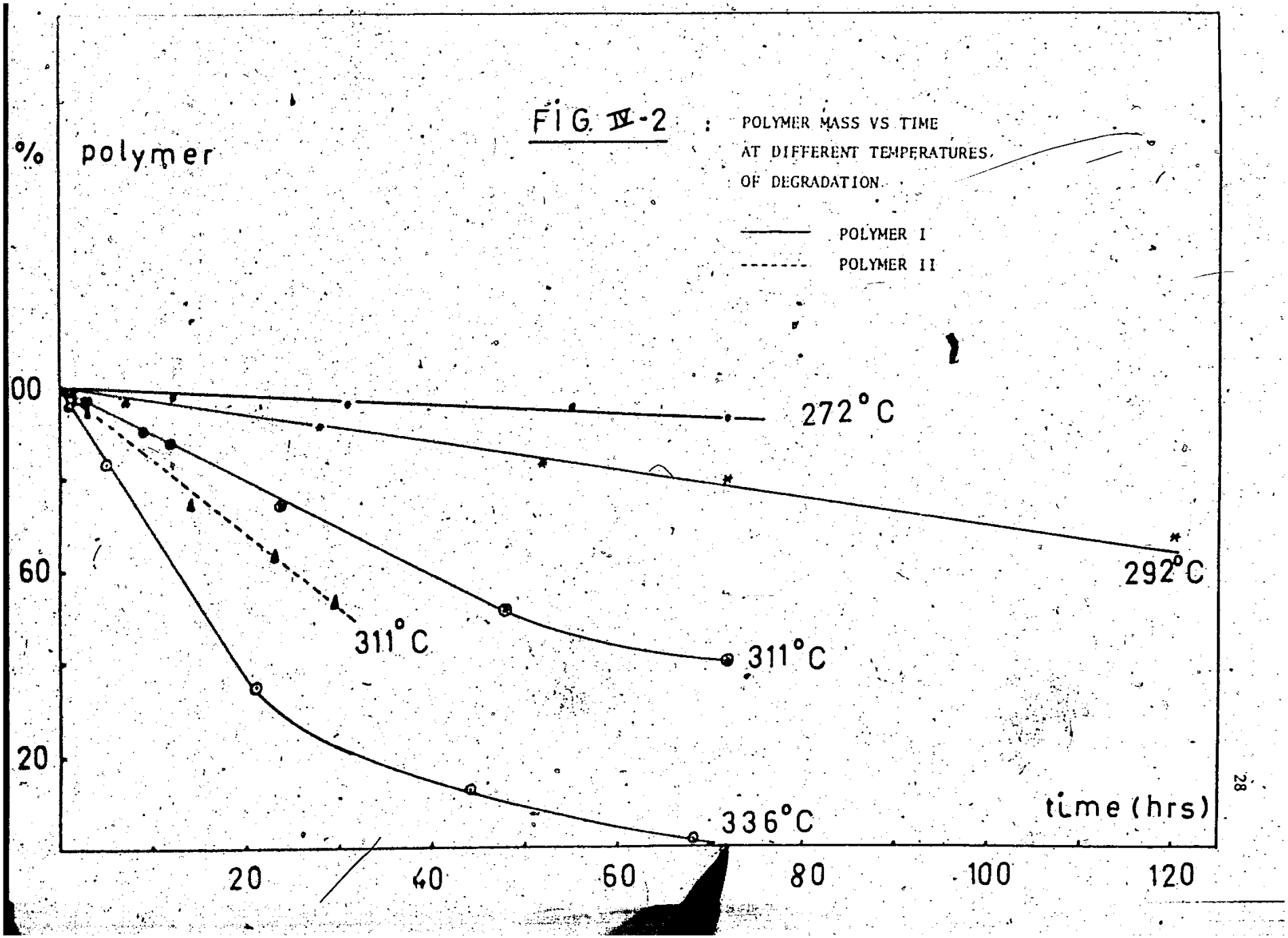
FIG. IV-2 : POLYMER MASS VS TIME AT DIFFERENT TEMPERATURES OF DEGRADATION.
POLYMER I
POLYMER II
% polymer
00
60
20
272°C
292°C
311°C
311°C
336°C
time (hrs)
20
40
60
80
100
120

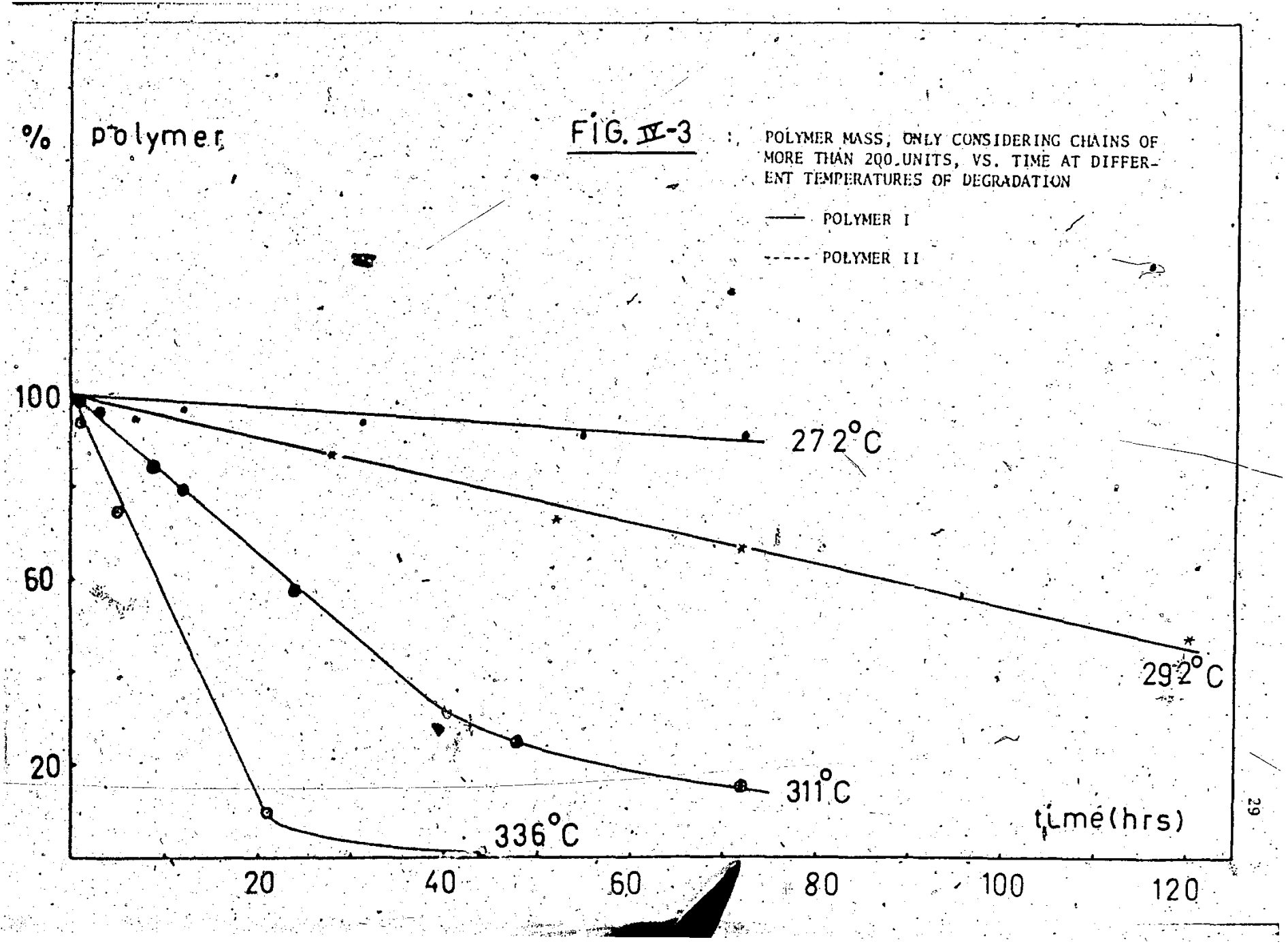

FIG. IV-3 : POLYMER MASS, ONLY CONSIDERING CHAINS OF MORE THAN 200 UNITS, VS. TIME AT DIFFERENT TEMPERATURES OF DEGRADATION

—— POLYMER I

----- POLYMER II

(311°C, 336°C). Based on the initial idea of solely depolymerization the following two kinetic schemes were developed:

1. **Instantaneous Unzipping**

This model, which adequately describes the thermal degradation of poly (methylmethacrylate), consists of the following process: as soon as a chain gets initiated, monomer units come off very quickly until the whole chain has disappeared. The kinetic equations are:

$$\frac{dP_n}{dt} = - k_{dp} P_n$$

from which $P_n = P_{no} \exp (- k_{dp} t)$

The monomer production, or decrease in polymer mass can be found from:

$$\frac{dM}{dt} = - \frac{d \sum_{n=2}^{\infty} n P_n}{dt} = k_{dp} \left(\sum_{n=2}^{\infty} n P_{no} \right) \exp (-k_{dp} t) \qquad (1)$$

The moment equations are:

$$\sum_{n=2}^{\infty} n P_n = \left(\sum_{n=2}^{\infty} n P_{no} \right) \exp (- k_{dp} t) \qquad (2)$$

$$\sum_{n=2}^{\infty} P_n = \left(\sum_{n=2}^{\infty} P_{no} \right) \exp (- k_{dp} t) \qquad (3)$$

$$\sum_{n=2}^{\infty} n^2 P_n = \left(\sum_{n=2}^{\infty} n^2 P_{no} \right) \exp (- k_{dp} t) \qquad (4)$$

where P_n is the number of chains, in grammoles per liter reacting mixture, containing n monomer units. From (2), (3) and (4) follows

$$\bar{r}_n = \bar{r}_{no} \quad \text{and} \quad \bar{r}_w = \bar{r}_{wo}$$

the number and weight average chain lengths remain constant during degradation.

A quick look at the results for polystyrene degradation shows that this model cannot be valid for the two experimental facts:

(a) $\bar{r}_n$ and $\bar{r}_w$ fall rapidly with time

(b) the polymer mass does not vary exponentially with time but rather linearly (figure IV-2).

2. Slow Unzipping

This process consists of monomer units splitting off at the chain ends. The kinetic equations are:

$$\frac{dP_n}{dt} = k_{dp} (P_{n+1} - P_n)$$

$$\frac{d\left(\sum_{n=2} P_n\right)}{dt} = k_{dp} \left(\sum_{n=2} P_{n+1} - \sum_{n=2} P_n\right)$$

$$\text{or} \quad \frac{d\left(\sum_{n=2} P_n\right)}{dt} = -k_{dp} P_2 \qquad (5)$$

$$-\frac{dM}{dt} = \frac{d\left(\sum_{n=2} n P_n\right)}{dt} = k_{dp} \left(\sum_{n=2} n P_{n+1} - \sum_{n=2} n P_n\right)$$

$$= -k_{dp} \left(P_2 + \sum_{n=2} P_n\right) \qquad (6)$$

Assuming in the first stage of degradation the number of dimers to be negligible ($P_2 \simeq 0$) then from equations (5) and (6)

$$\sum_{n=2}^{\infty} P_n = \sum_{n=2}^{\infty} P_{no}$$

and

$$\frac{d\left(\sum_{n=2}^{\infty} n P_n\right)}{dt} = - k_{dp} \sum_{n=2}^{\infty} P_{no}$$

or

$$\sum_{n=2}^{\infty} n P_n = \sum_{n=2}^{\infty} n P_{no} - \left(\sum_{n=2}^{\infty} P_{no}\right) k_{dp} t$$

$$\bar{r}_n = \bar{r}_{no} - k_{dp} t \qquad (7)$$

In the same manner the weight-average chain length can be derived to give:

$$\bar{r}_w = \bar{r}_{wo} - 2 k_{dp} t \qquad (8)$$

Equation (6) could explain the linear variation of polymer mass versus time as the total number of particles remains constant in the early periods of degradation and also the reduction in rate at higher degrees of degradation, when the total number of polymer chains starts falling due to their disappearance as monomer.

As more experimental information became available however, some facts indicated the inconsistency of this model.

(a) $\bar{r}_n$ and $\bar{r}_w$ do not vary linearly with time but rather exponentially (see figures IV-4, IV-5, IV-6)

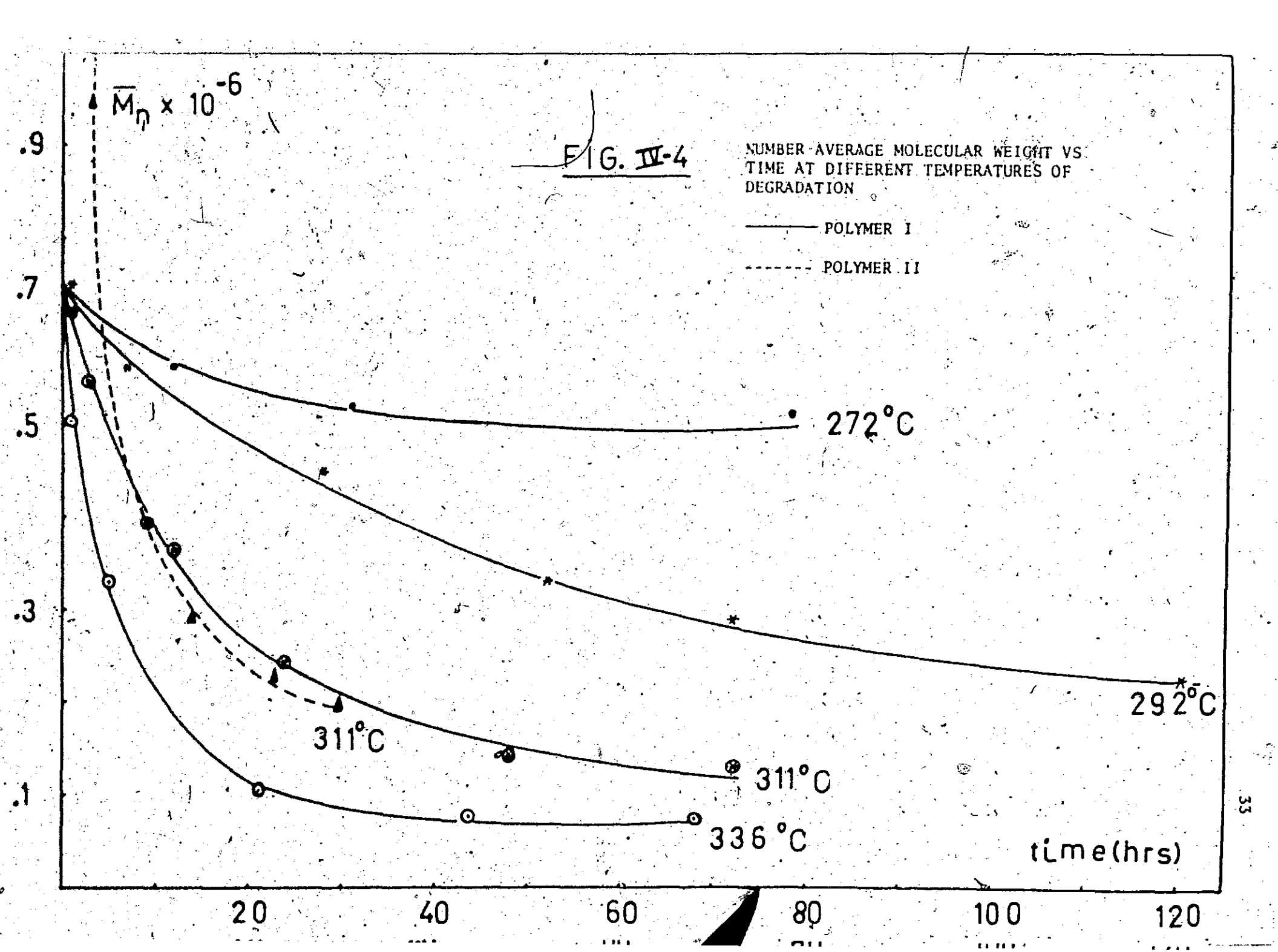

FIG. IV-4

NUMBER-AVERAGE MOLECULAR WEIGHT VS TIME AT DIFFERENT TEMPERATURES OF DEGRADATION

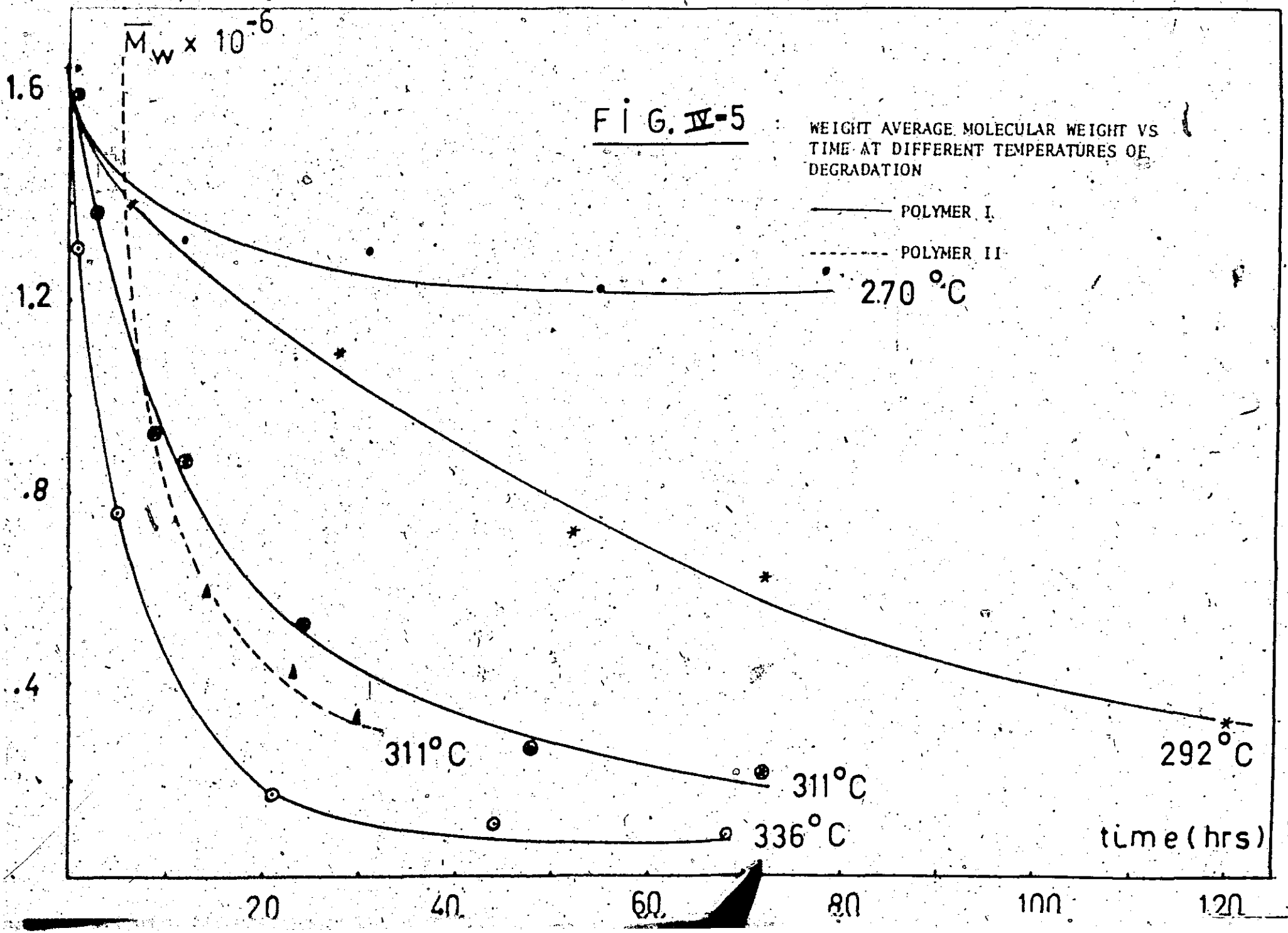

FIG. IV-5

WEIGHT AVERAGE MOLECULAR WEIGHT VS TIME AT DIFFERENT TEMPERATURES OF DEGRADATION

——— POLYMER I

- - - - - - - POLYMER II

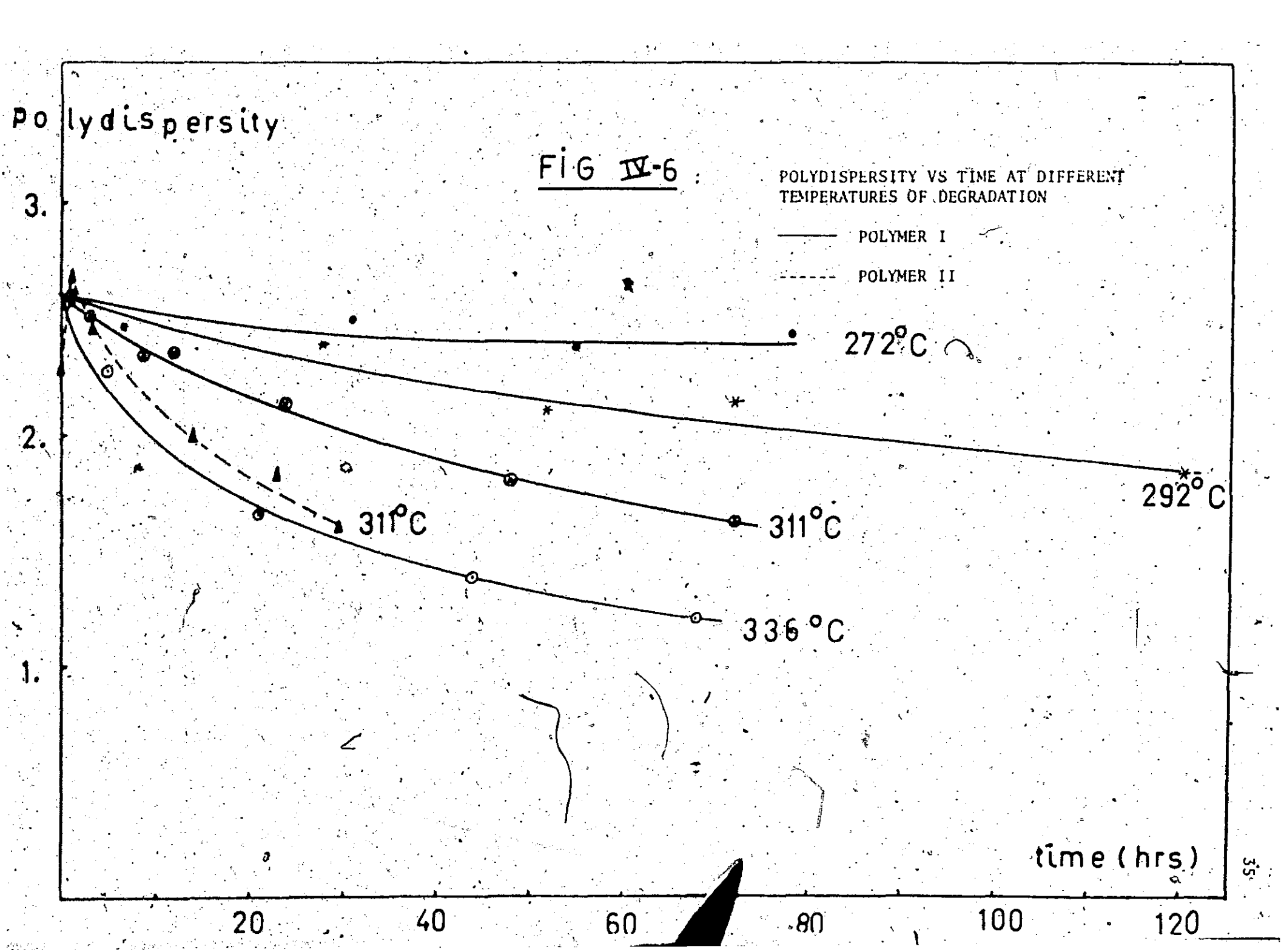
Polydispersity
FIG IV-6 :
POLYDISPERSITY VS TIME AT DIFFERENT TEMPERATURES OF DEGRADATION
POLYMER I
POLYMER II
272°C
292°C
311°C
311°C
336°C
3.
2.
1.
time (hrs)
20
40
60
80
100
120

(b) from equation (6) follows that in order for the drop in polymer mass to be proportional with time, the total number of chains, $\sum_{n=2}^{\infty} P_n^*$, should remain constant with time. This could be considered to be so, within experimental error, (figure IV-7) for 272°C and 292°C, but becomes rather dubious for 311°C and 336°C, for which the total number of particles almost doubles, before decreasing.

Without the simplifying assumption that the amount of dimers is negligible in the early stages of the reaction, equation(6) cannot explain the straight line behaviour of the drop in polymer mass. This model was thus ruled out.

---

*for the method of calculation of $\sum_{n=2} P_n$, see appendix 4.

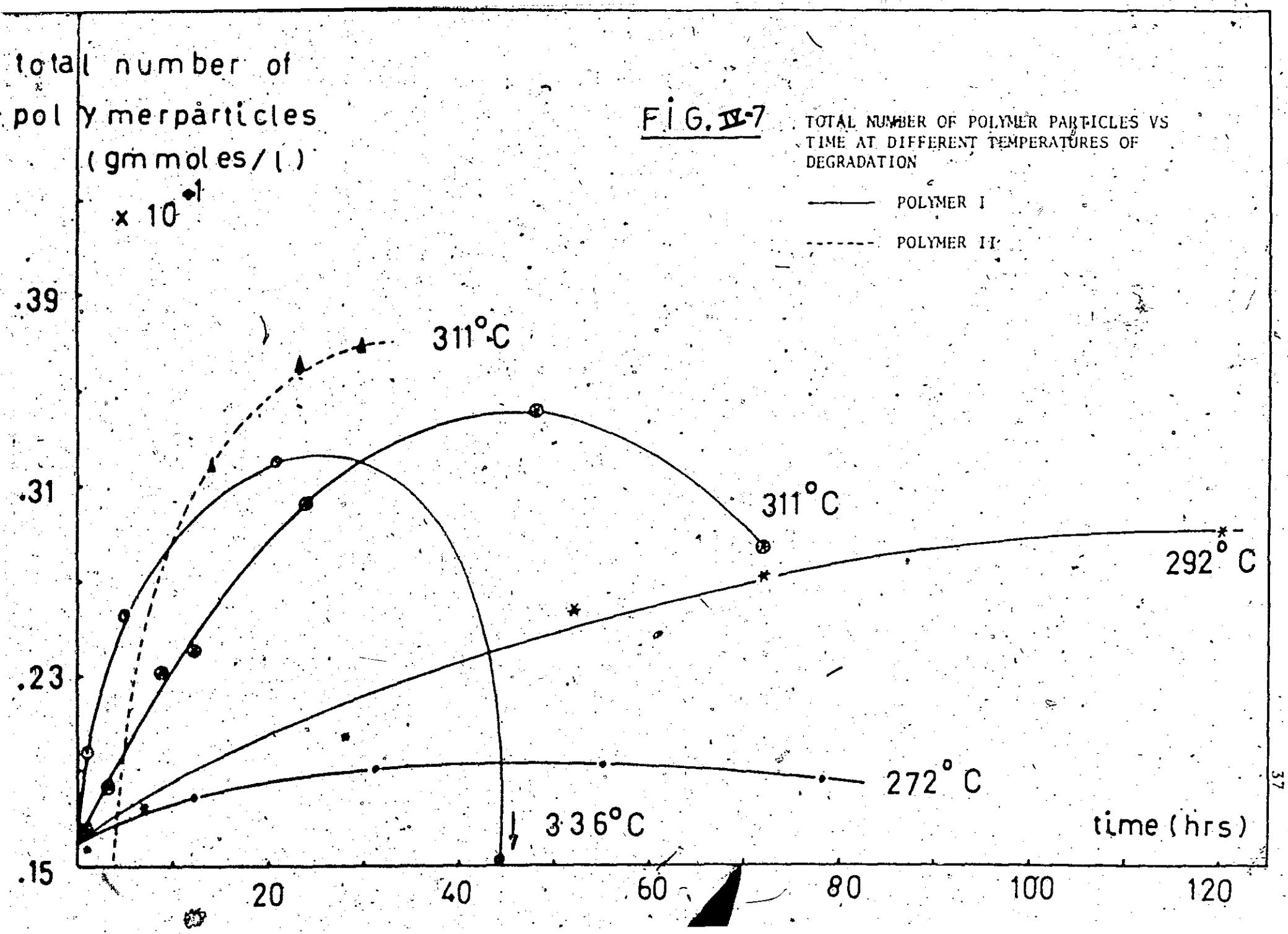

FIG. IV-7 TOTAL NUMBER OF POLYMER PARTICLES VS TIME AT DIFFERENT TEMPERATURES OF DEGRADATION

——— POLYMER I

------- POLYMER II

IV-3 Degradation, a reversible process?

Since a pure unzipping model could never explain the degradation products as reported in the literature (42% styrene and 58% low molecular weight fraction) we had to consider the possibility of a reverse process, probably polymerization, going on simultaneously during the thermal degradation.

To test this hypothesis, samples with different extents of degradation were kept for 40 hours at 168°C to see if any repolymerization was taking place. The amount of volatile fraction, and molecular weight averages were measured before and after the repolymerization experiment.

TABLE IV-1

SAMPLE NO.	BEFORE/AFTER REPOLYMERIZATION	VOLATILE FRACTION (%)	$\bar{M}_n$	$\bar{M}_w$	P.D.
I	before	9.26	51,415	126,432	2.459
	after	9.24	46,608	122,136	2.620
II	before	50.25	14,102	28,049	1.99
	after	53.85	12,985	25,120	1.93
III	before	84.17	8,250	11,490	1.39
	after	83.32	8,409	12,126	1.44

From table IV-1 no particular trend can be observed, the data before and after repolymerization are considered to be within experimental error. The molecular weight distributions were also superimposed, no noticeable difference was remarked. The possibility of large scale repolymerization was then ruled out. Most probably the repolymerization

of the monomer formed is inhibited by other degradation products. This seems to indicate that no equilibrium for the different temperatures is involved in the degradation process. Other experimental observations will confirm this assumption, e. g. superposition of the decrease of average molecular weights at different temperatures, when plotted versus extent of volatilization (see further).

IV-4 Importance of the extent of degradation

Before trying out another model it was thought interesting to plot average molecular weights, and total number of polymer particles against the more comparable extents of volatilization. This showed amazing results.

Plotted against extent of volatilization the number (figure IV-8), weight-average molecular weights (figure IV-9) and total number of particles (figure IV-10) superimposed on one curve for the different degradation temperatures investigated. This has the following consequences:

1. A polymer with given molecular weight distribution will degrade along the same path of molecular weight distributions, no matter the degradation temperature. The temperature will only influence the time at which a certain degree of degradation will be reached.
2. For a given polymer the activation energy of the constants involved in the degradation process must be the same, since different

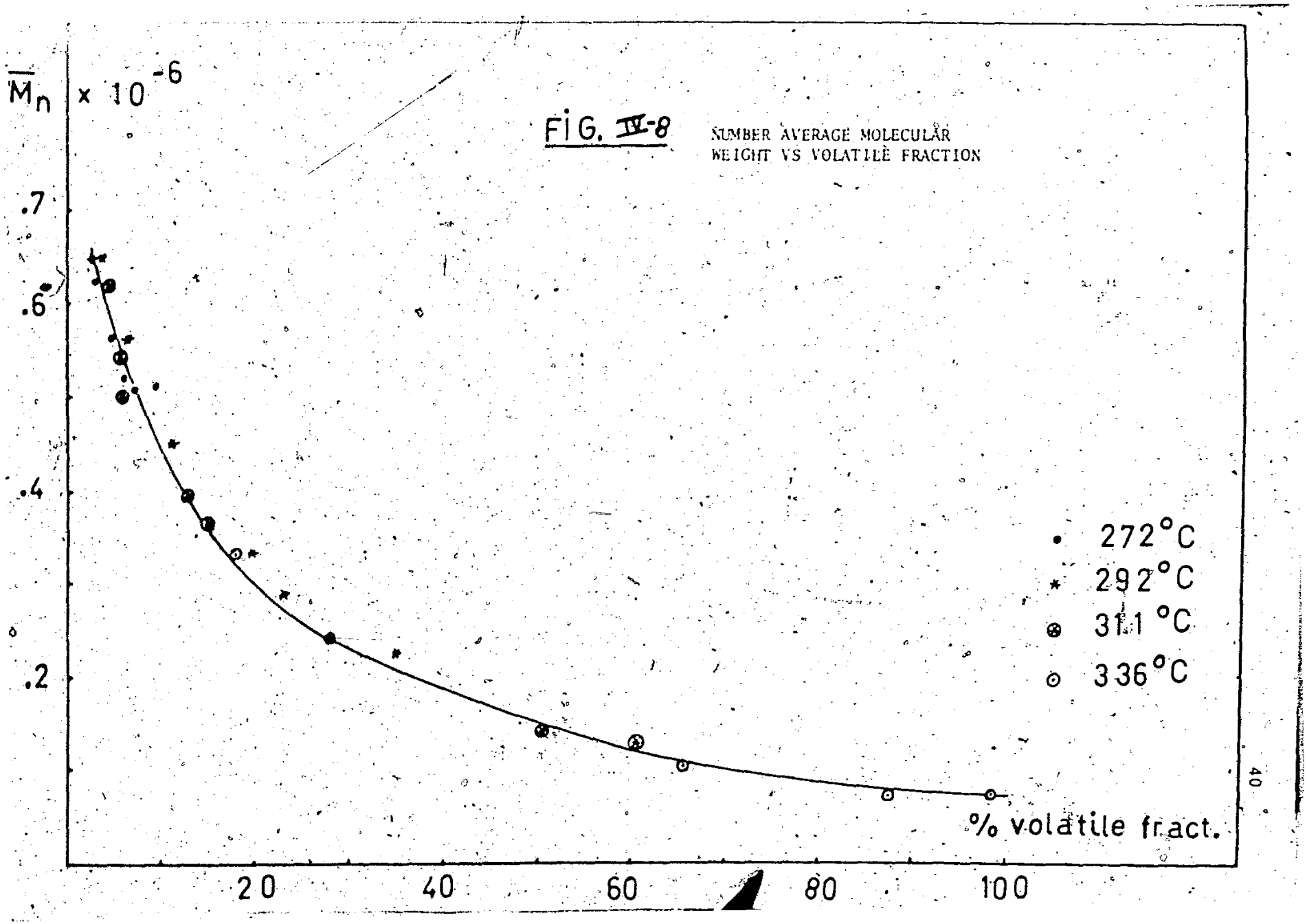

FIG. IV-8 NUMBER AVERAGE MOLECULAR WEIGHT VS VOLATILE FRACTION

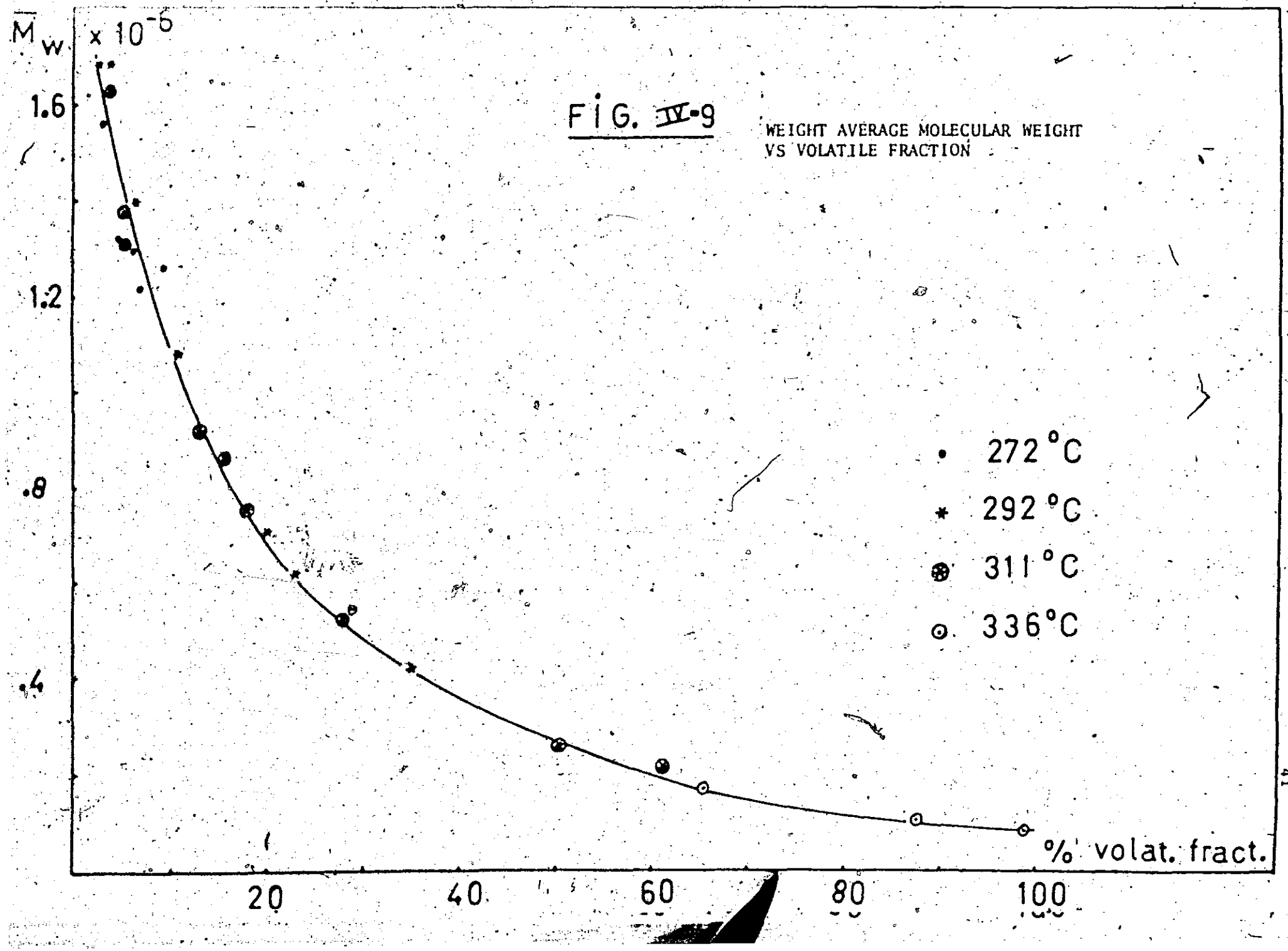

FIG. IV-9

WEIGHT AVERAGE MOLECULAR WEIGHT VS VOLATILE FRACTION

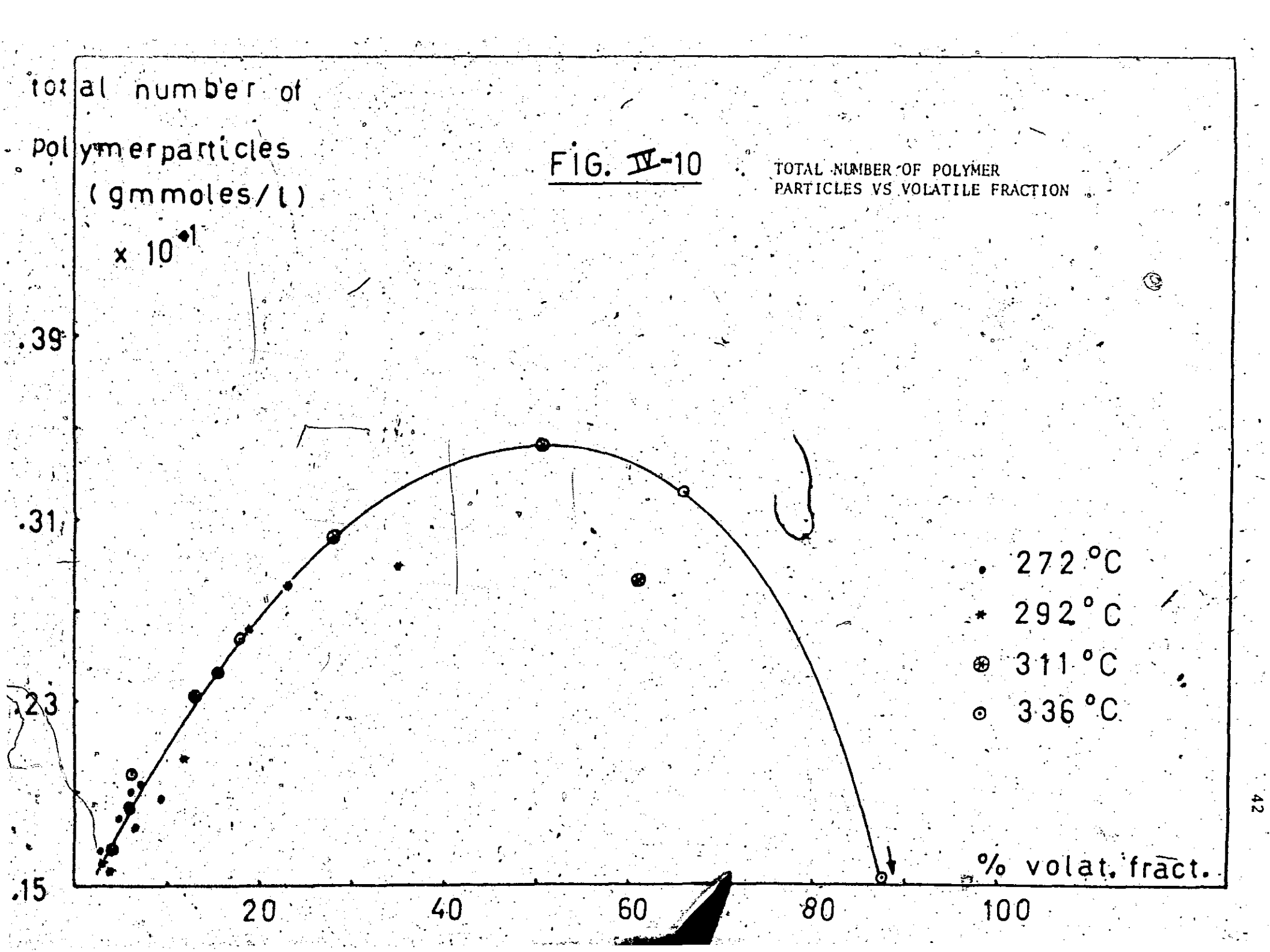

FIG. IV-10 TOTAL NUMBER OF POLYMER PARTICLES VS VOLATILE FRACTION

activation energies would make the coinciding of the different curves rather unlikely.

3. This means also that if we write the kinetic equations, describing the degradation mechanism, as a function of the degree of volatilization, the kinetic constants should be independent of temperature. In order to obtain Arrhenius plots these kinetic equations will have to be expressed again as functions of time, or simply the reaction constants multiplied by the rates of volatilization at the corresponding temperatures. This will become clearer in the development of the following models. What is very important however is that this implies that the rates of volatilization at the different temperatures fit an Arrhenius equation. That this is so can be seen from figure IV-11. The rates of volatilization obtained from figure IV-1 are

TABLE IV - 2

TEMPERATURE (^{o}C)	RATE OF VOLATILIZATION (sec^{-1})
270	2.31×10^{-7}
292	7.81×10^{-7}
311	2.72×10^{-6}
336	8.27×10^{-6}

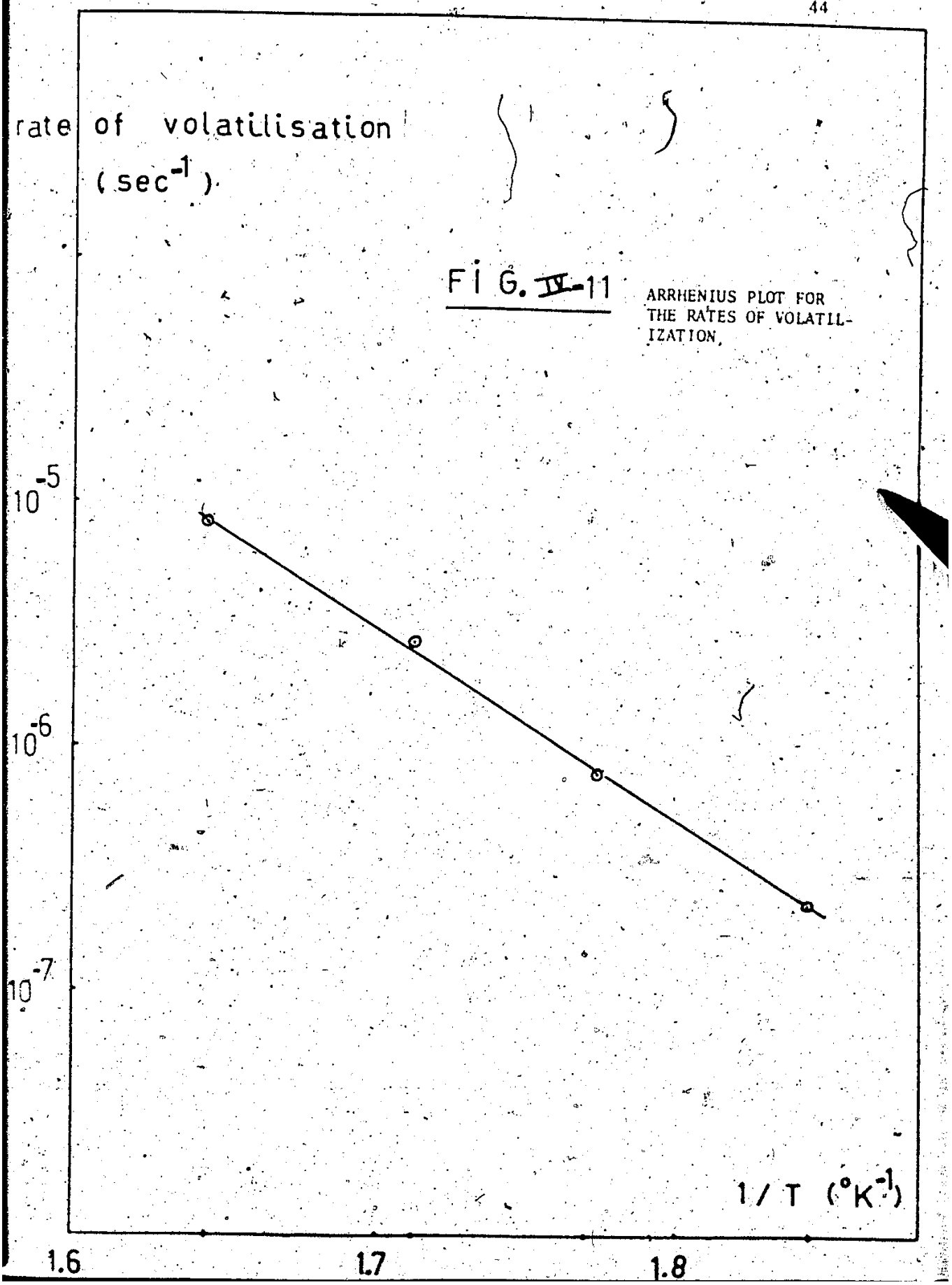

FIG. IV-11 ARRHENIUS PLOT FOR THE RATES OF VOLATILIZATION.

The activation energy, governing the degradation process of our polymer can now already be forecasted from this Arrhenius plot: 34.2 kcal/mole.

4. Although no equilibrium studies were carried out, the superposition of these curves seems to indicate that at the different temperatures the degradation will go all the way to almost complete decomposition, and apparently no equilibrium for the different temperatures is involved. The only variable is the time at which this endpoint will be reached, the higher the temperature the sooner. This is not in complete agreement with Odian [17], who states the ceiling temperature (T_c) for pure styrene to be 310°C.

NOTE:

(a) It should be interesting to investigate if the same degradation path will also be followed by a polymer with completely different molecular weight distribution. To test this out figures IV-8 and IV-9 were plotted more generally in figure IV-12 and IV-13 in order to be used as possible master curves.

(b) This superposition of the degradation curves for different temperatures was already ment-

FIG. IV-12

NUMBER AVERAGE MOLECULAR WEIGHT RATIO VS VOLATILE FRACTION (NOT INCLUDING INITIAL MONOMER)

——— POLYMER I

- - - - - - - POLYMER II

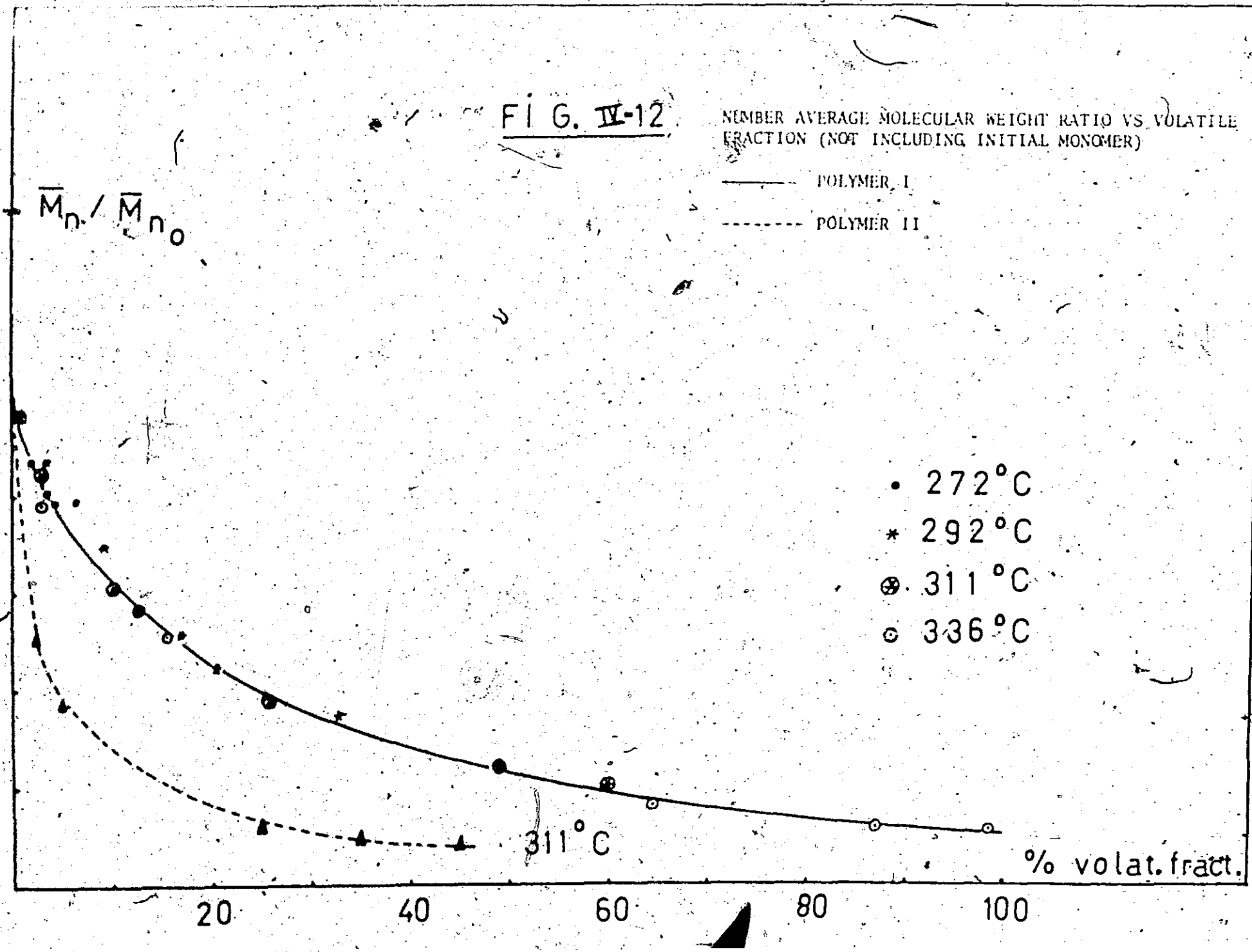

FIG. IV-13 : WEIGHT AVERAGE MOLECULAR WEIGHT RATIO VS VOLATILE FRACTION (NOT INCLUDING INITIAL MONOMER)

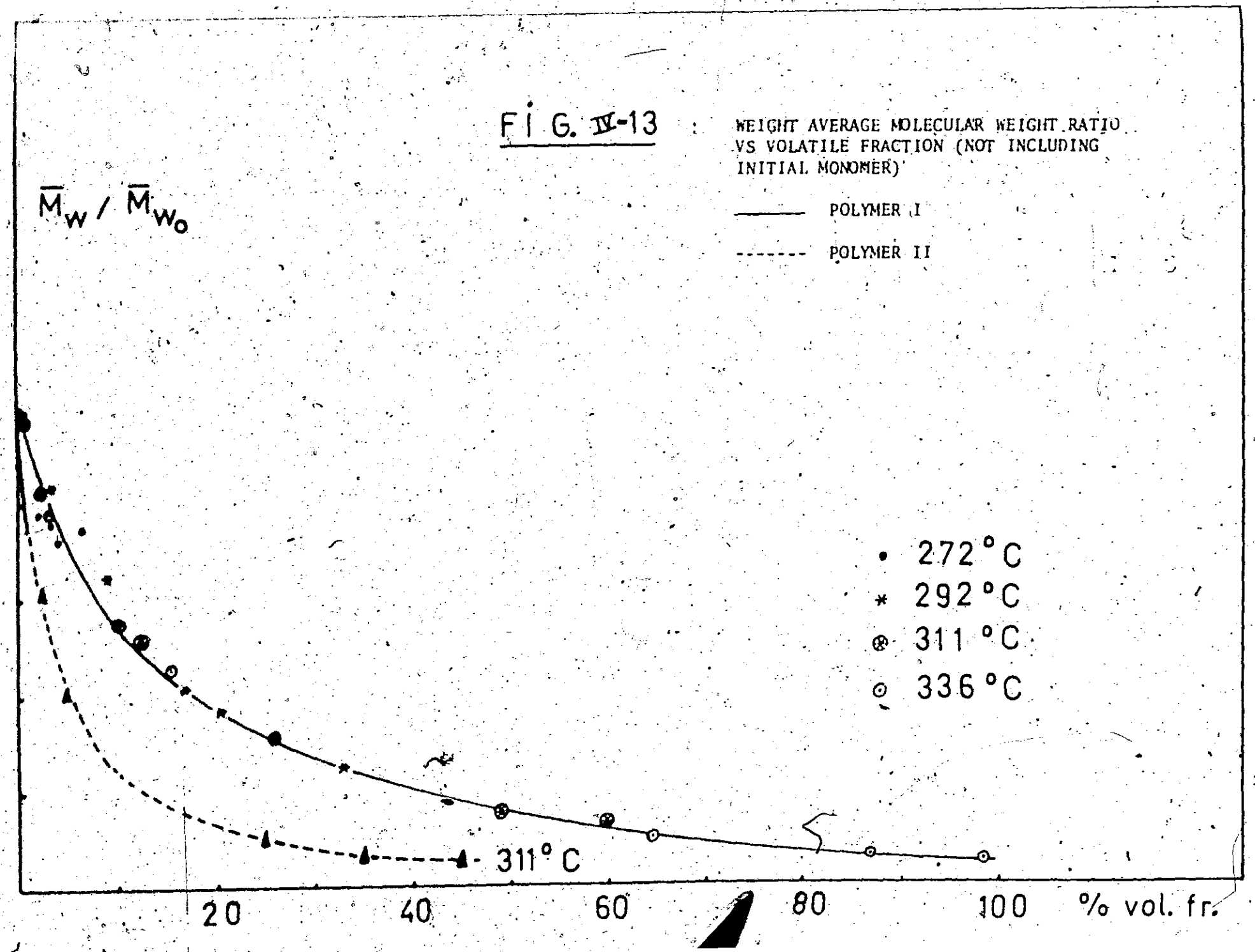

ioned by Grassie and Kerr[4] for a temperature range between 280 and 300°C. That this would be valid for the broader range, 270°C to 340°C, has never been reported.

(c) The activation energy found here can be compared with those obtained by other investigators:

Jellinek (2) : 44.7 kcal/mole

Madorsky (3) : 55 kcal/mole

(d) The superposition at the different temperatures is excellent for the weight average molecular weight, good for the number average and reasonable for the total number of particles. This corresponds with the relative influence of the lower molecular weight tail on these quantities.

IV-5 Model 2: Unzipping with depropagation constant function of chain length

At this moment in the investigations it was still believed the number of particles to remain constant before decreasing. This assumption could be considered within experimental error at 270°C and 292°C (figure IV-7), and is also valid at 311°C and 336°C when only polymer chains larger than 600 units are considered (figure IV-14 to figure IV-18).

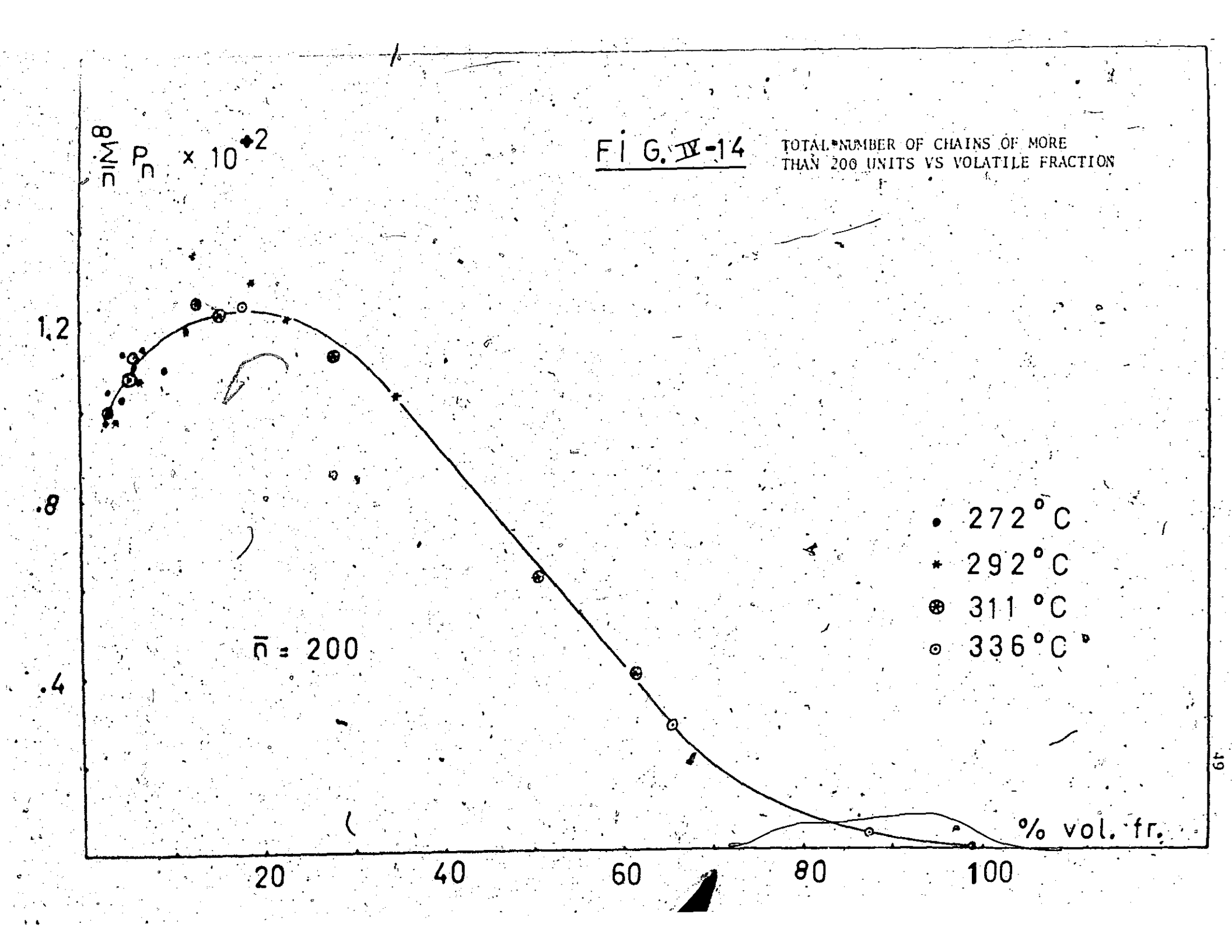
FIG. IV-14
TOTAL NUMBER OF CHAINS OF MORE THAN 200 UNITS VS VOLATILE FRACTION
$\Sigma W_n P_n \times 10^{+2}$
1.2
.8
.4
$\bar{n} = 200$
272 °C
292 °C
311 °C
336 °C
% vol. fr.
20
40
60
80
100

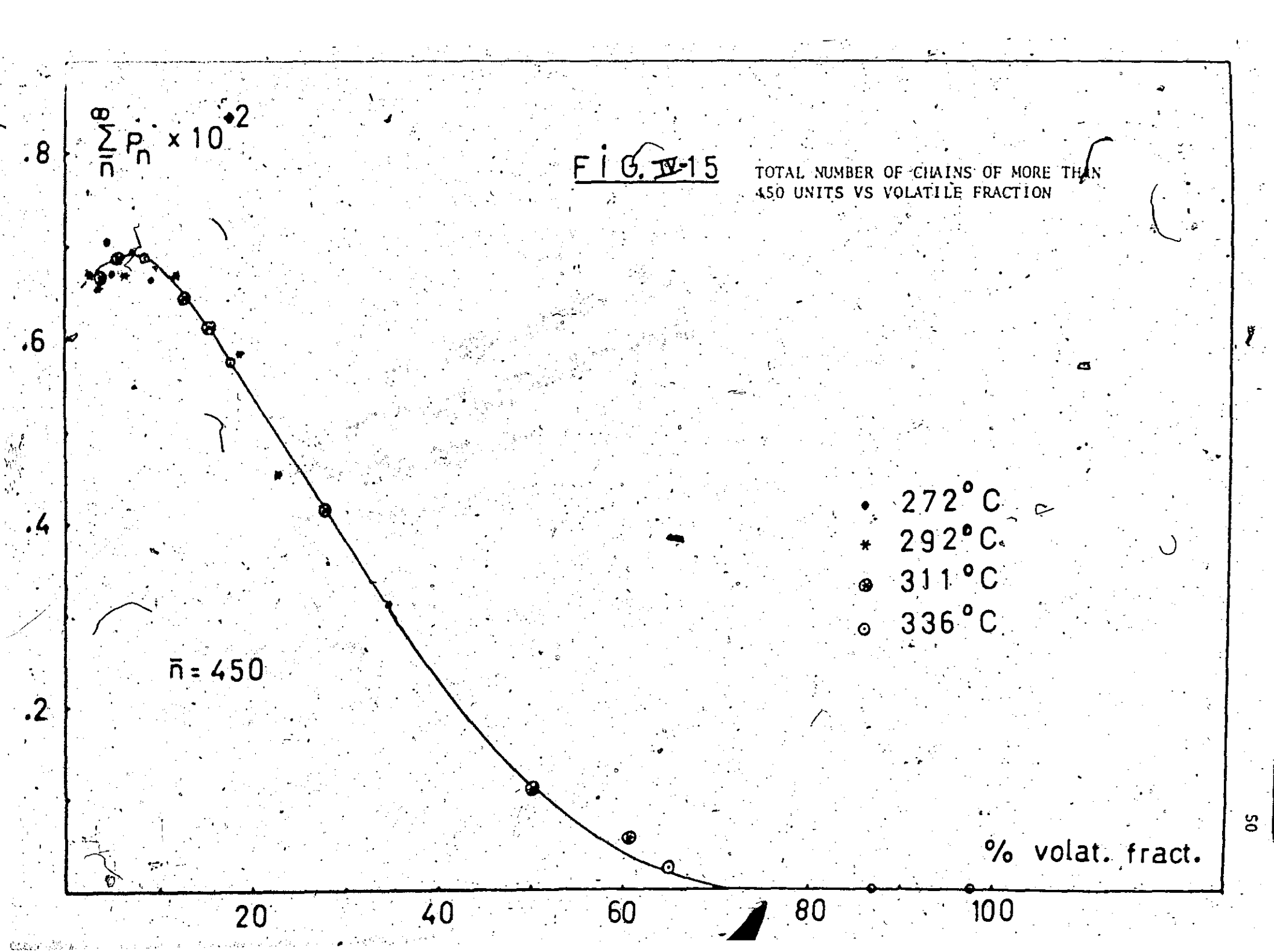

FIG. IV-15 TOTAL NUMBER OF CHAINS OF MORE THAN 450 UNITS VS VOLATILE FRACTION

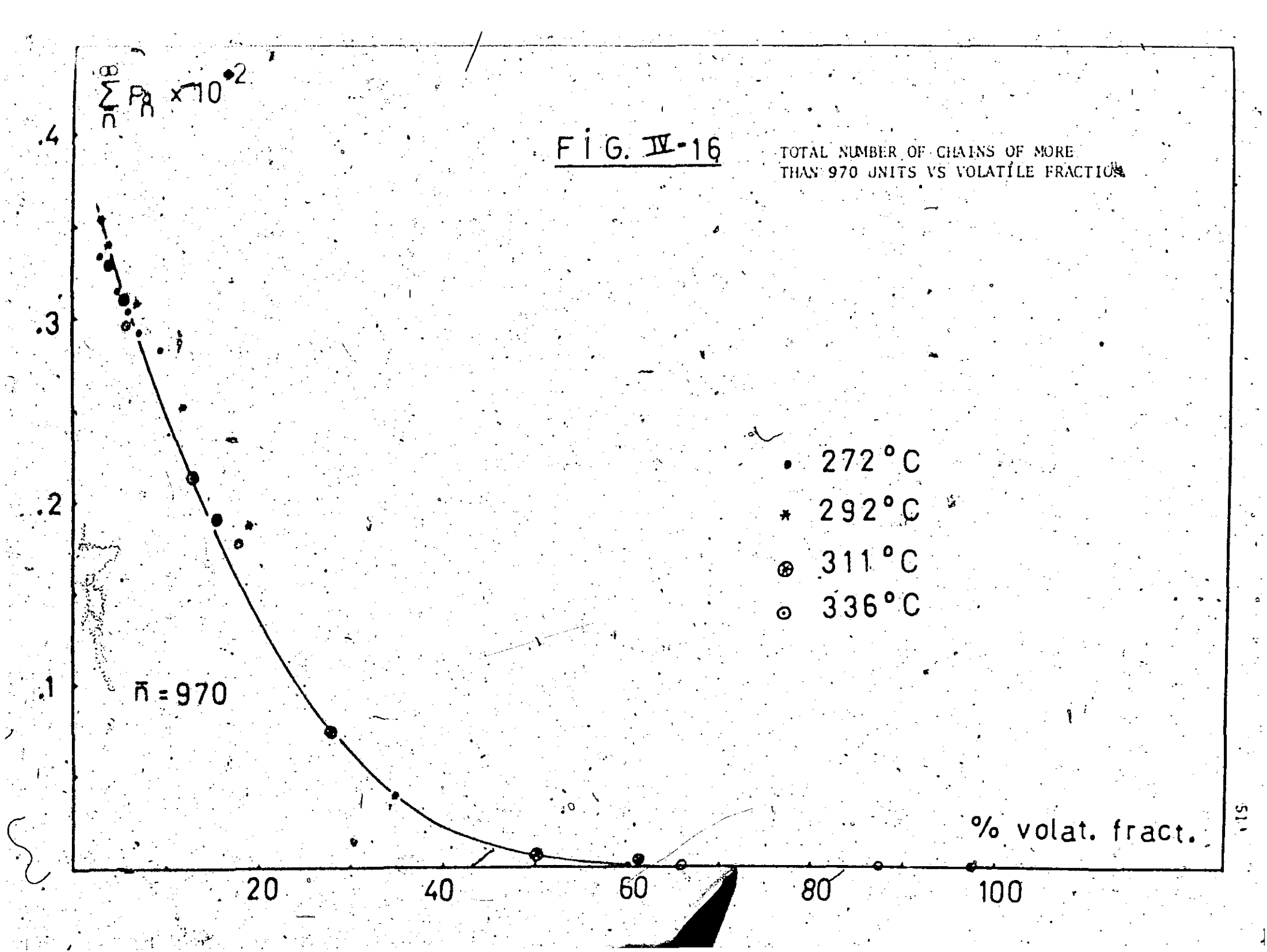
$\sum_{n}^{\infty} P_R \times 10^{+2}$
FIG. IV-16
TOTAL NUMBER OF CHAINS OF MORE THAN 970 UNITS VS VOLATILE FRACTION
.4
.3
.2
.1
$\bar{n} = 970$
• 272 °C
* 292 °C
⊛ 311 °C
⊙ 336 °C
% volat. fract.
20
40
60
80
100

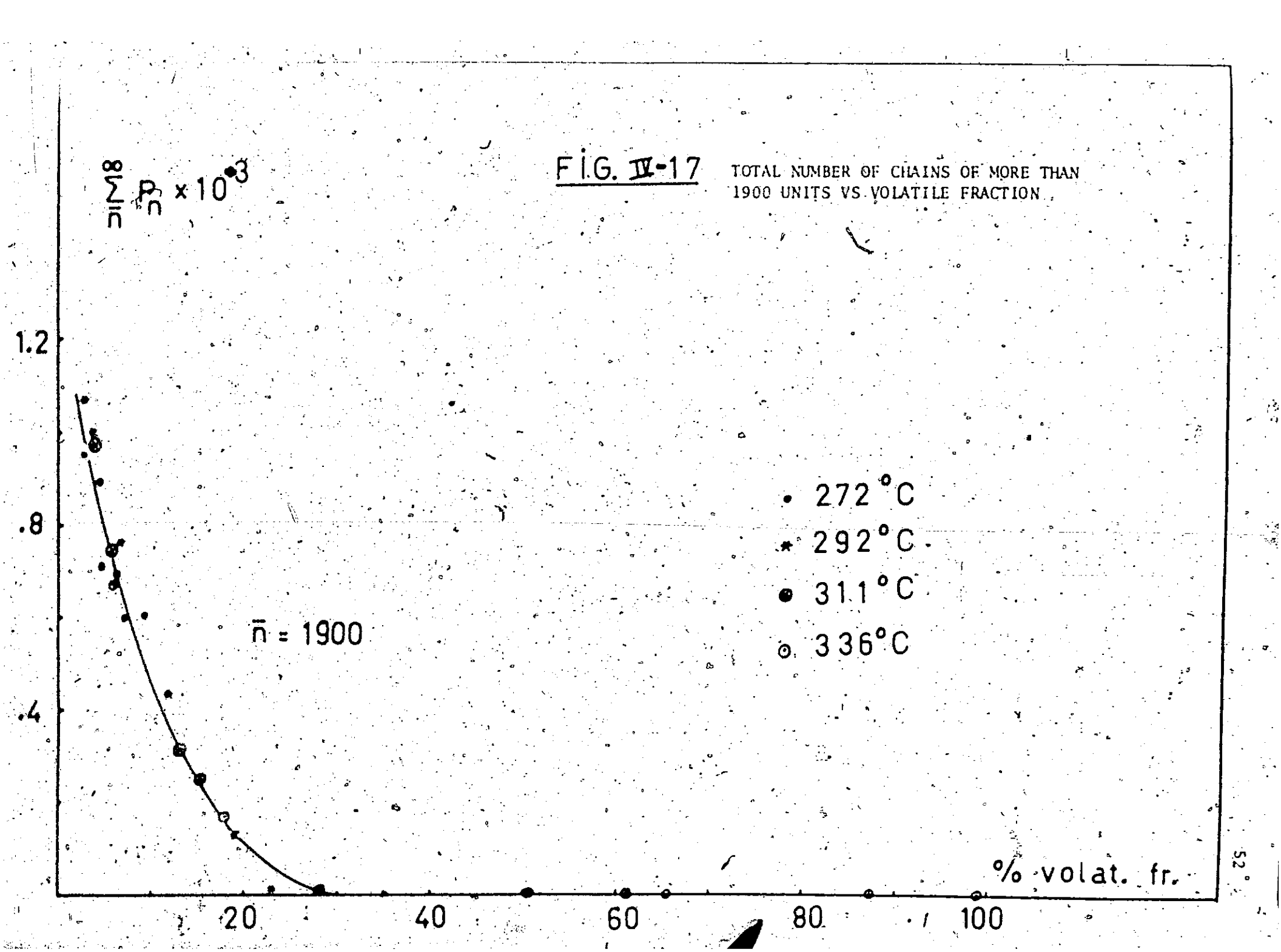

FIG. IV-17 TOTAL NUMBER OF CHAINS OF MORE THAN 1900 UNITS VS VOLATILE FRACTION.

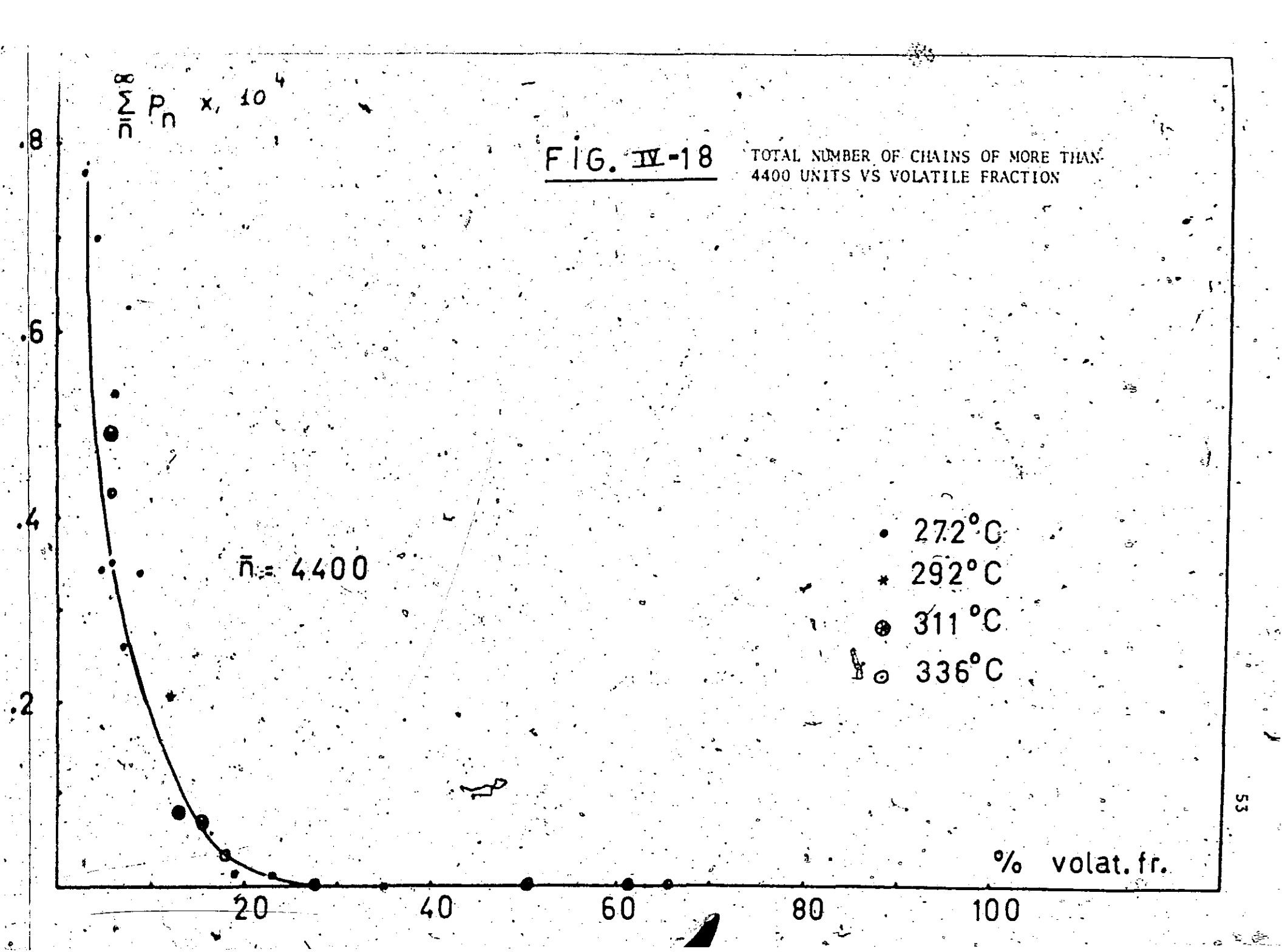

FIG. IV-18 TOTAL NUMBER OF CHAINS OF MORE THAN 4400 UNITS VS VOLATILE FRACTION

Although the hypothesis of a depropagation constant being a function of chain length seems rather unreasonable from the point of view that above a certain minimum length any chain end should be the same, and in each case the same carbon-carbon bond is broken, this is already reported earlier in the literature. Wall and coworkers [7] explored the rates of volatilization for monodisperse polystyrenes particularly in the low molecular weight range (up to M.W. 64,000). They found the collision factor from the Arrhenius equation to be increasing with increasing molecular weight. They also reported a drop in the activation energy from 49 kcal at higher molecular weights (>24,500) to 24 kcal for a 3,400 molecular weight sample.

This model was also favoured since it could not only explain the linear variation of volatile fraction with time, but also the exponential drop in the average molecular weights.

Different ways of investigating the chain length dependence of k_{dp} were then explored. We will restrict ourselves to the easiest and most obvious method. Another way of obtaining the different k_{dp}'s is given in Appendix 2.

The equation for a chain containing n monomer units is:

$$\frac{dP_n}{dt} = k_{dp}(n)(P_{n+1} - P_n)$$

Summing from $\bar{n}$ to infinity:

$$\frac{d \sum_{n=\bar{n}}^{\infty} P_n}{dt} = \sum_{n=\bar{n}}^{\infty} k_{dp}(n)(P_{n+1} - P_n)$$

Working out the summation on the right handside, we get:

$$\frac{d \sum_{n=\bar{n}}^{\infty} P_n}{dt} = - k_{dp}(\bar{n}) \; P_{\bar{n}} \qquad (9)$$

So, if in equation (9) we start the summation at different $\bar{n}$ or chain length, we obtain the corresponding $k_{dp}(\bar{n})$. The use of equation (9) requires taking the derivatives of $\sum_{n=\bar{n}}^{\infty} P_n$ verus time for the different temperatures of degradation. This would be rather difficult since not enough experimental data are available at each temperature. Using master curves however and expressing equation (9) as a function of % volatile materials, x, gave the ideal solution:

$$\frac{d \sum_{n=\bar{n}}^{\infty} P_n}{dx} = - k_{dp} \; P_{\bar{n}} \; / \; dx/dt$$

$$\text{from which } k_{dp}(\bar{n}) = - \frac{d \sum_{n=\bar{n}}^{\infty} P_n}{dx} \; \frac{1}{P_{\bar{n}}} \; \frac{dx}{dt} \qquad (10)$$

Plots of $\sum_{n=\bar{n}}^{\infty} P_n$ versus x for different $\bar{n}$ are given in figures IV-14-18. The Arrhenius plots for the $k_{dp}(\bar{n})$ are on figure IV-19. Parallel lines, proving a constant energy of activation, were obtained for molecular weights between 60,000 and 290,000. The corresponding data are given in tableform in appendix 3. Outside this molecular weight range deviating results were obtained. For molecular weights lower than 60,000 this is probably due to the influence of the rise in total number of particles at lower extents of volatilization (see figure IV-14-15). For molecular weights larger than 290,000 the decline in $\sum P_n$ with x is so steep that accurate slope measurements become dubious. The activation energies obtained

FIG. IV-19 ARRHENIUS PLOT OF THE DEPROPAGATION CONSTANTS FOR VARYING CHAIN LENGTHS

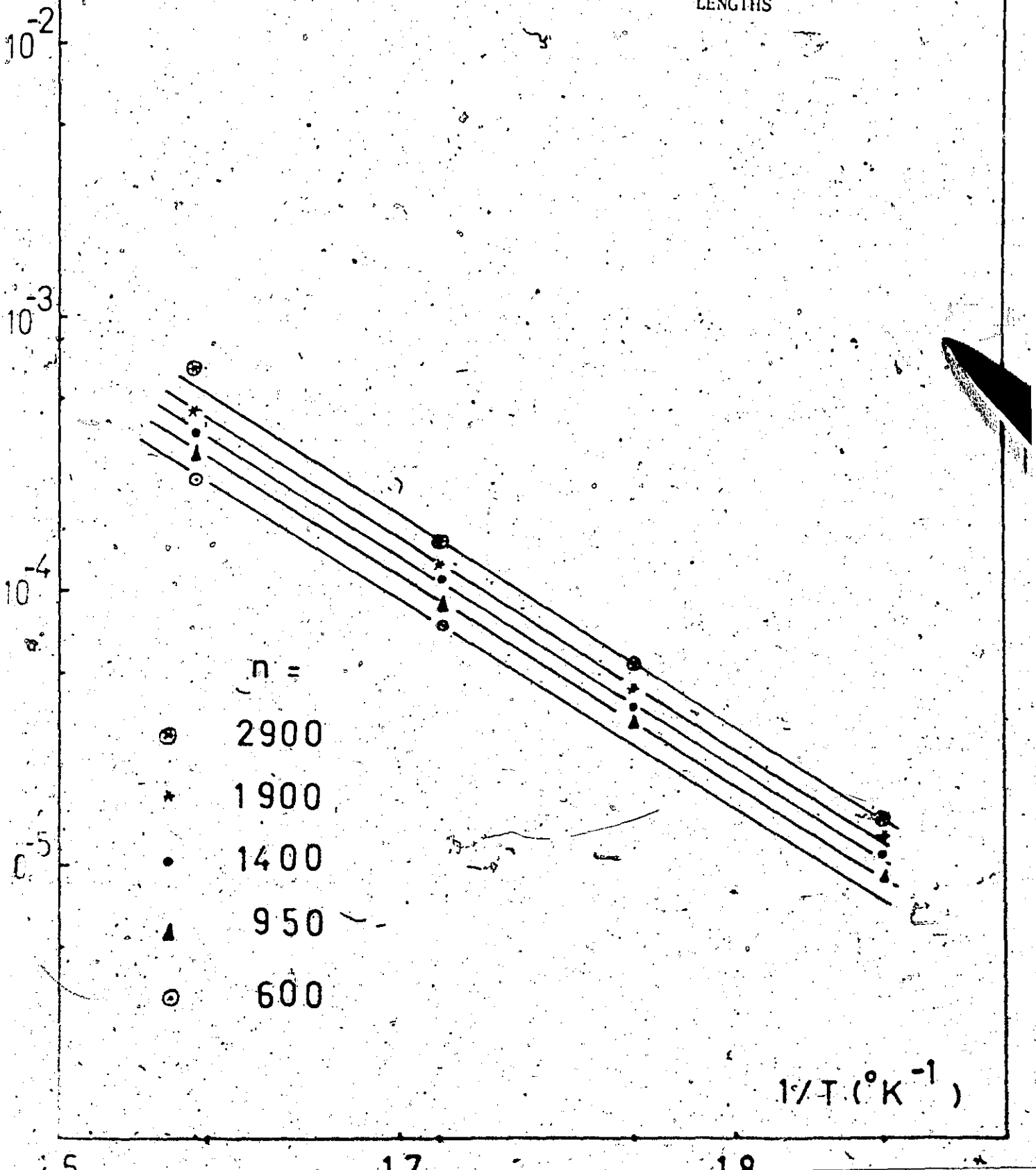

were 34.254 kcal/mole, almost identical as measured earlier. Plotting the collision factors A from the Arrhenius equation versus M.W. gave a straight line (figure IV-20), from which the following relation A(M.W.) was derived:

$$A = .346 \times 10^{9} \ln (M.W./12,000) \qquad (11)$$

The extrapolation of this relation to lower molecular weights (<60,000) gives the apparent rather strange result that for molecular weights lower than 12,000 k_{dp} should become zero. This is not so unreasonable, when we look at figures IV-12 and IV-13: the average molecular weights are leveling off around molecular weight 8,000! A very small value for the depropagation constant would be more logical, but, in each case the contribution of volatile materials of chains smaller than around 120 units should be negligible compared with the total production of these materials.

Remark that the same $k_{dp}(\bar{n})$ should have been obtained using equation (10) in the form:

$$\bar{k}_{dp}(\bar{n}) = - \frac{d \sum_{n=\bar{n}}^{\infty} P_n}{dx} \frac{1}{P_{\bar{n}}} \qquad (11)$$

The $\bar{k}_{dp}(\bar{n})$ from this equation is only function of chain length, the values corresponding to each degradation temperature can be found by multiplying by the appropriate rates of volatilization.

To check the adequacy of this model we used equation (6) in the form:

$$- \frac{dM}{dt} = \frac{d \sum_{n=2}^{\infty} n P_n}{dt} = \sum_{n=2}^{\infty} k_{dp}(n) P_n$$

Left and right hand side of this equation should yield the same number.

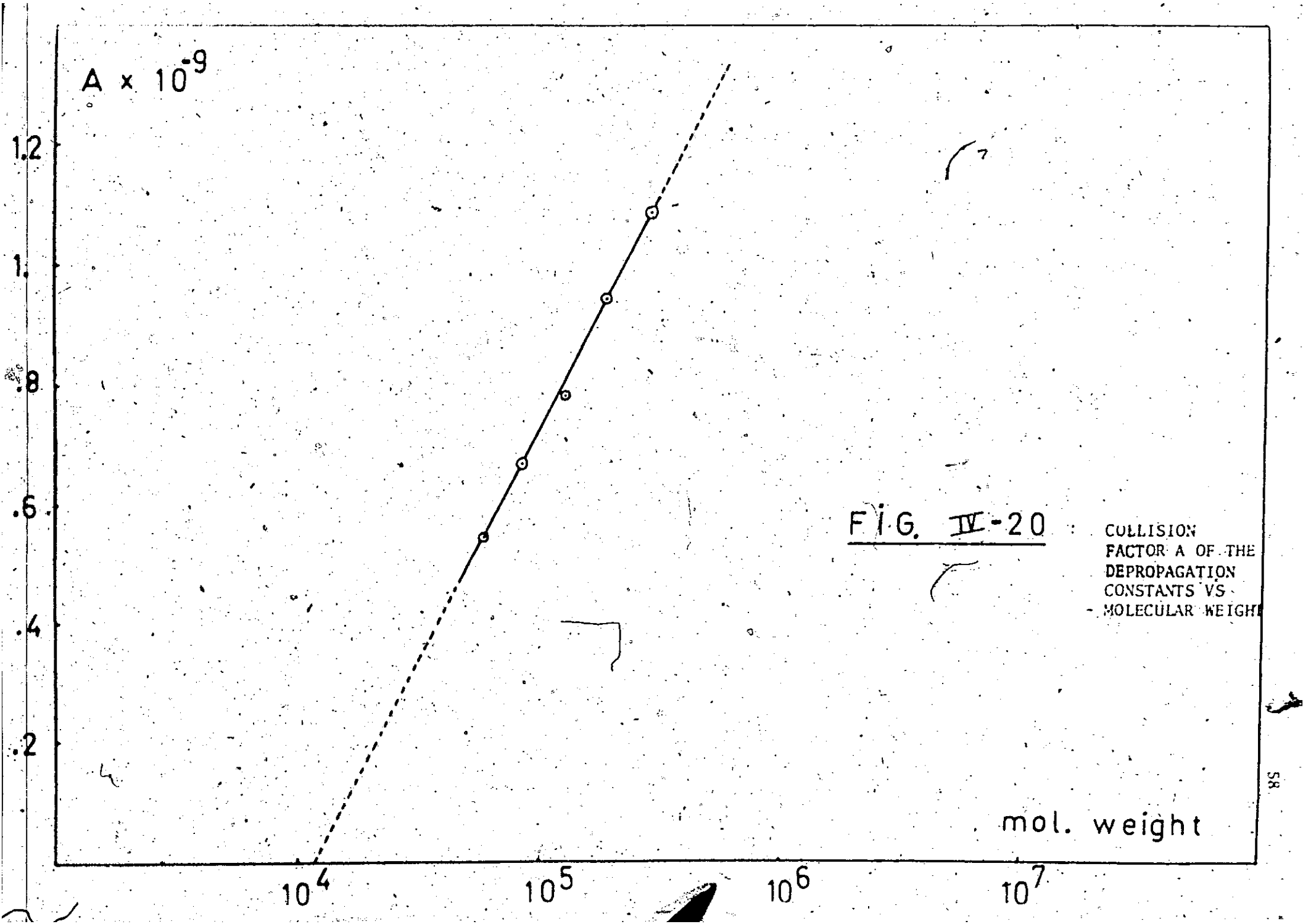

FIG. IV-20 : COLLISION FACTOR A OF THE DEPROPAGATION CONSTANTS VS MOLECULAR WEIGHT

The results are given in table IV-3. In this table it can be seen that $\frac{d\left(\sum_{n=2}^{\infty} n P_n\right)}{dt}$ is larger than $\sum_{n=2}^{\infty} k_{dp}(n) \cdot P_n$, in other words the decrease in polymer mass ($\Sigma n P_n$) with time cannot be explained solely through unzipping, even with a chain length dependent depropagation constant. An additional mechanism for polymer breakdown should be considered. This mechanism should also account for the rise in total number of particles in the earlier stages of degradation. This will be the starting point for models 3 and 4.

IV-6 Introduction to Scission

A point of discussion in the literature is whether scission takes place at "weak" links or at random.

Cameron and Kerr [9] showed that when thermally polymerized polystyrenes are decomposed, the rate at which bonds are broken randomly satisfies the relationship:

$$\alpha = \beta + kt \qquad (12)$$

where α is the degree of degradation or fraction of bonds broken per molecule at time t and can be expressed as

$$\frac{1}{DP_t} - \frac{1}{DP_o}$$

β is an apparent factor of thermolabile bonds in the polymer

k is a first order velocity constant for bond scission.

So it is assumed here that "weak" links break very rapidly at the onset of the reaction. Consequently, the presence and magnitude of an ordinate intercept in plots of α versus time will indicate the existence of any weak bonds.

Table IV-3

Temperature of Degradation	Time	$\frac{d\left(\sum_{n=2}^{\infty} n P_n\right)}{dt}$	$\sum_{n=2}^{\infty} k_{dp}(n) P_n$
270	0	$.231 \times 10^{-6}$	$.953 \times 10^{-7}$
	12	$.231 \times 10^{-6}$	$.991 \times 10^{-7}$
	31	$.231 \times 10^{-6}$	$.963 \times 10^{-7}$
	55	$.231 \times 10^{-6}$	$.979 \times 10^{-7}$
	72	$.231 \times 10^{-6}$	$.944 \times 10^{-7}$
292	0	$.781 \times 10^{-6}$	$.317 \times 10^{-6}$
	1	$.781 \times 10^{-6}$	$.317 \times 10^{-6}$
	7	$.781 \times 10^{-6}$	$.327 \times 10^{-6}$
	28	$.781 \times 10^{-6}$	$.336 \times 10^{-6}$
	52	$.781 \times 10^{-6}$	$.332 \times 10^{-6}$
	72	$.781 \times 10^{-6}$	$.303 \times 10^{-6}$
	120	$.781 \times 10^{-6}$	$.246 \times 10^{-6}$
311	1	$.272 \times 10^{-5}$	$.865 \times 10^{-6}$
	3	$.272 \times 10^{-5}$	$.896 \times 10^{-6}$
	9	$.272 \times 10^{-5}$	$.909 \times 10^{-6}$
	12	$.272 \times 10^{-5}$	$.888 \times 10^{-6}$
	24	$.272 \times 10^{-5}$	$.747 \times 10^{-6}$
	48	$.272 \times 10^{-5}$	$.396 \times 10^{-6}$
	72	$.1032 \times 10^{-5}$	$.264 \times 10^{-6}$
336	1	$.827 \times 10^{-5}$	$.307 \times 10^{-5}$
	5	$.827 \times 10^{-5}$	$.294 \times 10^{-5}$
	21	$.827 \times 10^{-5}$	$.622 \times 10^{-6}$
	44	$.163 \times 10^{-5}$	$.102 \times 10^{-6}$
	68	$.463 \times 10^{-6}$	$.175 \times 10^{-8}$

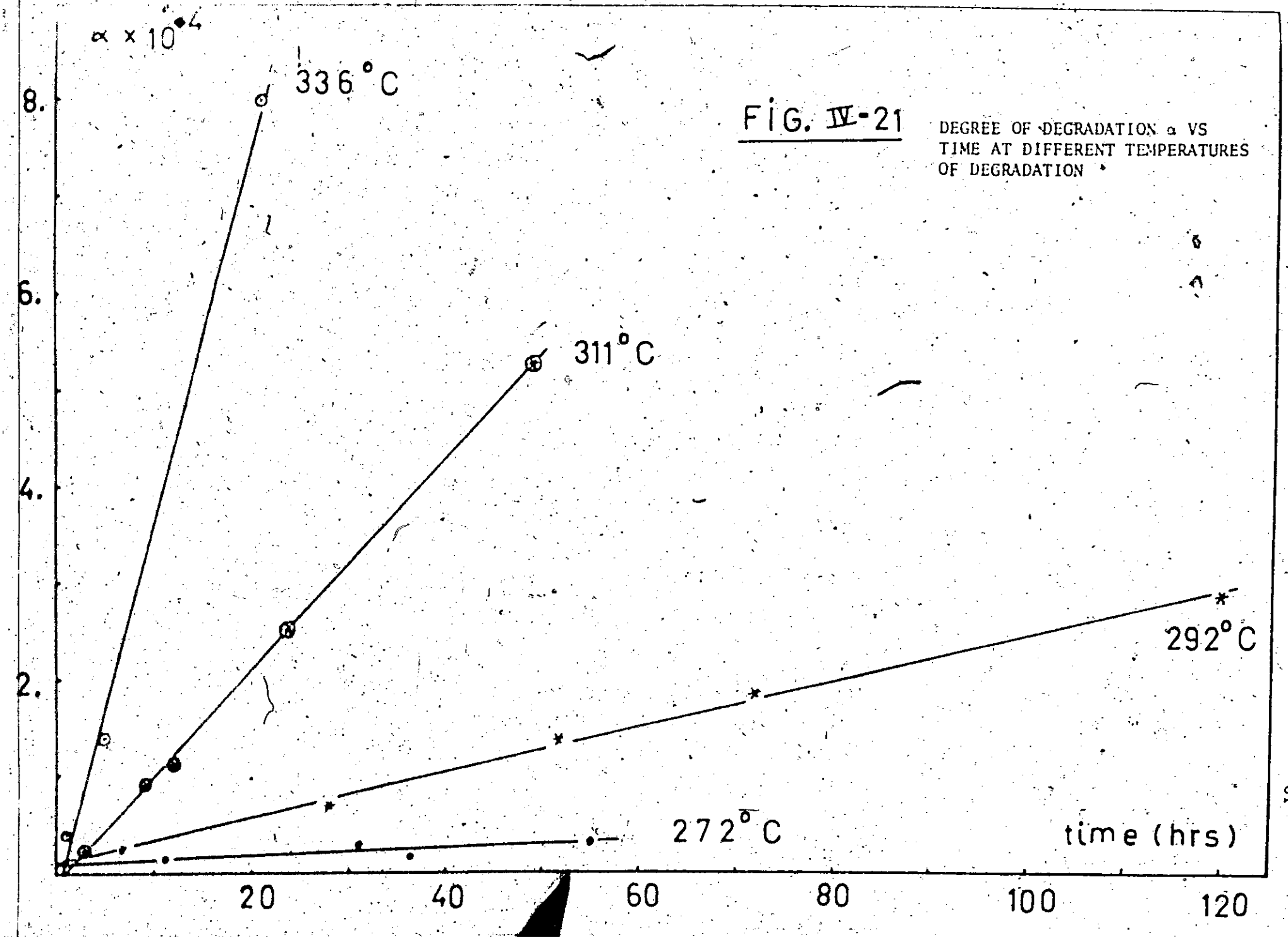

FIG. IV-21 DEGREE OF DEGRADATION α VS TIME AT DIFFERENT TEMPERATURES OF DEGRADATION

Equation (12) for our polymer is shown in figure IV-21. No intercept is found, so "weak" links (structural or due to oxygen) can almost be ruled out, and random-scission will have to be considered.

IV-7 Model 3: Random Scission and Depolymerization

In order to explain the increase in total number of particles random degradation will be introduced. This mechanism alone however can never account for the total production of volatile materials during the degradation [3]. Depolymerization also will have to be considered. According to this model the rate of breakage of bonds will be:

$$\frac{dN}{dt} = - k_s N - 2 k_{dp} \sum_{n=\bar{n}}^{\infty} P_n \qquad (13)$$

where N is the total number of bonds in chains containing more than $\bar{n}$ units.

With at the most a 1% error, we can approximate this total number of bonds by the total number of monomer units in the system. Equation (13) becomes then

$$\frac{d \sum_{n=\bar{n}}^{\infty} n P_n}{dt} = - k_s \sum_{n=\bar{n}}^{\infty} n P_n - 2 k_{dp} \sum_{n=\bar{n}}^{\infty} P_n \qquad (14)$$

Equation (14) describes the evolution of polymermass as a function of time. A similar equation can be written for the number of polymer particles

$$\frac{d \sum_{n=\bar{n}}^{\infty} P_n}{dt} = - 2 k_{dp} P_{\bar{n}} - k_s \sum_{n=\bar{n}}^{\infty} P_n + 2 k_s \sum_{n=\bar{n}}^{\infty} \sum_{i=n}^{\infty} P_{i+2} \qquad (15)$$

Equation (14) in terms of x:

$$\frac{d \sum_{n=\bar{n}}^{\infty} \bar{n} P_n}{dx} = \bar{k}_s \sum_{n=\bar{n}}^{\infty} \bar{n} P_n - 2 \bar{k}_{dp} \sum_{n=\bar{n}}^{\infty} P_n \qquad (16)$$

As mentioned before $\bar{k}_s$ and $\bar{k}_{dp}$ in equation (16) will be independent of temperature. They are found using a least squares fit on the experimental data. Again we state the importance of the transformation to x, more experimental points become available and make the least squares fit more accurately.

Scission and depropagation constants found are given in table IV-4

TABLE IV - 4

$\bar{n}$	$\bar{k}_s$ (x^{-1})	$\bar{k}_{dp}$ (x^{-1})
2	.6771	$.9867 \times 10^{2}$
200	.2143	$.5900 \times 10^{3}$
600	.7767	$.261 \times 10^{4}$
1,900	.5499	$.1910 \times 10^{5}$

Remark that by using this method k_s and k_{dp} will automatically have the same activation energy. As an illustration the Arrhenius plots for k_s and k_{dp} are given for $\bar{n} = 1,900$ in figure IV-22.

From an analysis of the residuals the least squares fit can be considered to be very good: the residuals are small and randomly scattered.

FIG. IV-22

ARRHENIUS PLOT OF SCISSION AND DEPROPAGATION CONSTANTS FOR CHAINS LARGER THAN 1,900 UNITS

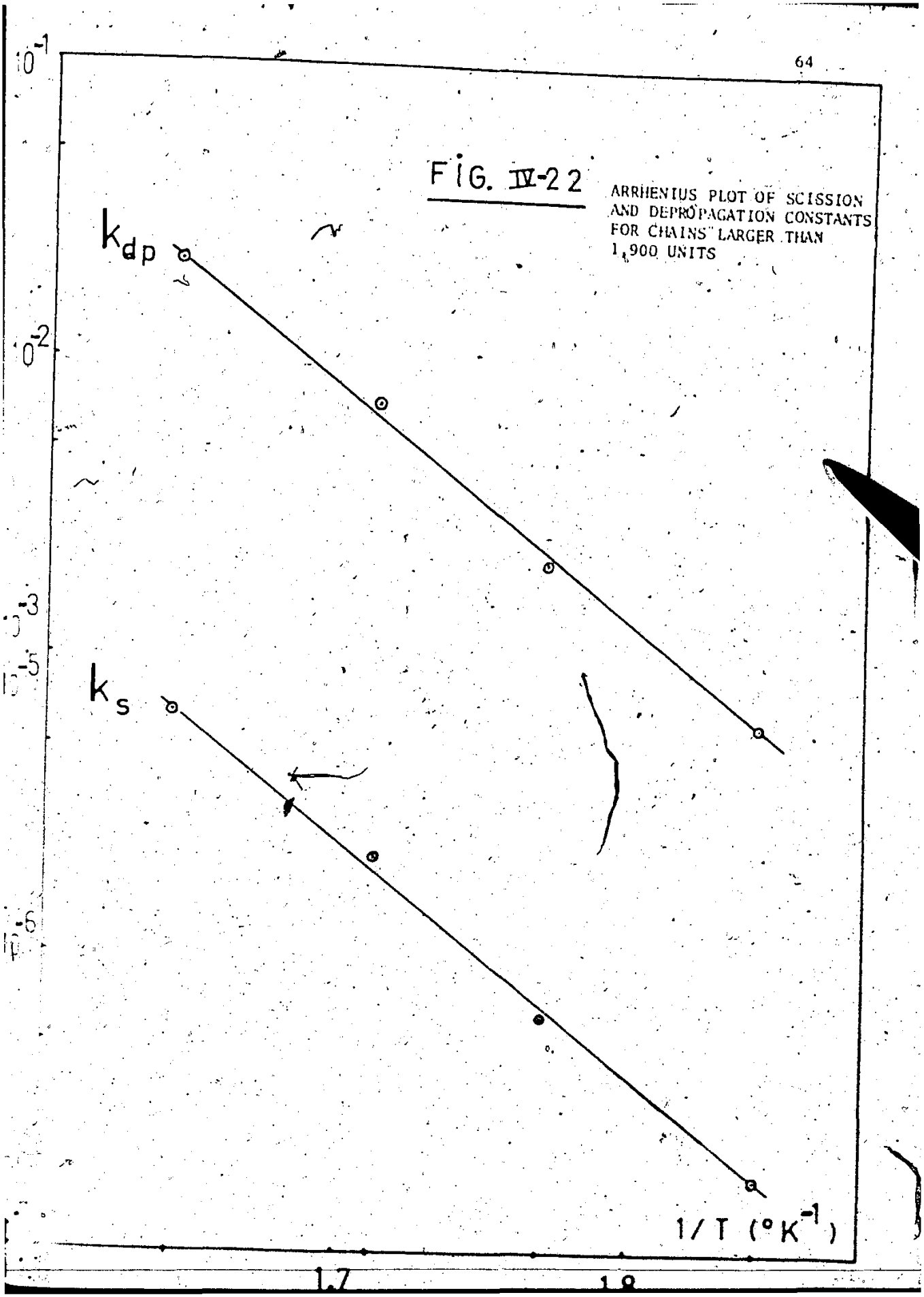

However to be consistent k_s and k_{dp} should be the same for different n. As can be seen from table IV-4, this is surely not the case for k_{dp}.

At this point no conclusions can be made, however, about the validity of the model. A quick look at the correlation matrix for k_s and k_{dp} shows a high negative correlation (-.9940) between the two constants. This means that a number of combinations between k_s and k_{dp} can give an equally good fit. Another method to determine k_s and k_{dp} will have to be sought.

IV-8 Model 4: Random Scission

When we look back at equation (14) we can see that in the early stages of degradation, when the total number of particles is small, the depropagation term will be negligible compared with the scission term. At later stages depropagation will become dominant. This approach can also be found in the literature [3, 4]. So if we restrict ourselves to the scission part of the degradation, equation (14) becomes

$$\frac{d \sum_{n=\bar{n}}^{\bar{n}} n P_n}{dt} = - k_s \sum_{n=\bar{n}}^{\bar{n}} n P_n \qquad (17)$$

which can be integrated to give:

$$\sum_{n=\bar{n}}^{\bar{n}} n P_n = \sum_{n=\bar{n}}^{\bar{n}} n P_{n_o} \exp(-k_s t) \qquad (18)$$

Again equation (17) was converted to volatile fraction, x. The results obtained are given in table IV-5:

$\bar{n}$	$k_s(x^{-1})$	$k_s(sec^{-1}) \times 10^6$			
		270°C	292°C	311°C	336°C
1,900	13.25	3.06	10.7	36.4	109.7
600	4.75	1.10	3.72	12.9	39.3
200	1.80	.42	.88	3.1	9.35

To prove the validity of the transformation to x, we will compare the k_s obtained through two different methods:

Method I: k_s obtained from least squares fit of equation (18) on $\Sigma n P_n$ versus time data at different temperatures

Method II: k_s obtained from least squares search on

$$\frac{d \sum_{n=\bar{n}}^{\infty} n P_n}{dx} = - k_s \sum_{n=\bar{n}}^{\infty} n P_n \qquad (19)$$

and multiplying with the rates of volatilization at the different temperatures.

The results are shown in table IV-6, $\bar{n}$ = 1,900:

TABLE IV - 6

T (°C)	k_s (sec^{-1}) x 10^6	
	I	II
270	3.19	3.06
292	10.57	10.7
311	36.21	36.4
336	122.1	109.7

To determine to what extent the depropagation term in equation (16) is statistically significant or not, we used the "extra sum of squares" principle

$$F_\alpha (1, n-2) = \frac{(RSS1 - RSS2)}{RSS2/n-2}$$

where F is the value of the F-distribution corresponding to level of significance α

RSS1 is the residual sum of squares of the solely scission model, equation (19)

RSS2 is the residual sum of squares of the model combining scission and depropagation, equation (16)

n is the number of observations.

For both least squares fits the experimental observations were cut off at 52% degradation. Beyond this point an inclination in the straight line behaviour of the degradation curves is observed (fig. IV-1-3).

TABLE -IV - 7

$\bar{n}$	(1) RSS1	(2) RSS2	(3) $RSS2/_{n-2}$	(4)=(1)-(2)	$(4)/_{(3)}$	$F_{\alpha=.95}(1,n-2)$
190,000	$.3038\times10^{3}$	$.2719\times10^{3}$	$.1511\times10^{2}$	$.319 \times 10^{2}$	2.11	4.4139
60,000	$.1751\times10^{3}$	$.5468\times10^{2}$	.2878x10	$.120 \times 10^{3}$	41.69	4.3808
20,000	$.1512\times10^{3}$	$.1803\times10^{2}$	.9487	$.133 \times 10^{3}$	140.2	4.3808
2	$.4123\times10^{2}$	.1453x10	.0765	$.398 \times 10^{2}$	520.3	4.3808

From table IV-7 follows that neglection of volatile formation at these temperatures is only allowed for molecular weights larger than 190,000 figure IV-23 and figure IV-24 show equation (19) for $\bar{n}$ = 1,900 and $\bar{n}$ = 600 respectively as fitted to the experimental data: the fit is much better for the larger $\bar{n}$. This conclusion is in contradiction with Cameron and Kerr [9] who assumed that at temperatures between 280°C and 310°C depropagation was negligible.

To be consistent the scission constants from table IV-5 and IV-6 should be independent of $\bar{n}$, where as now they increase with increasing $\bar{n}$. This puts forward the possibility of a chain length dependence of k_s.

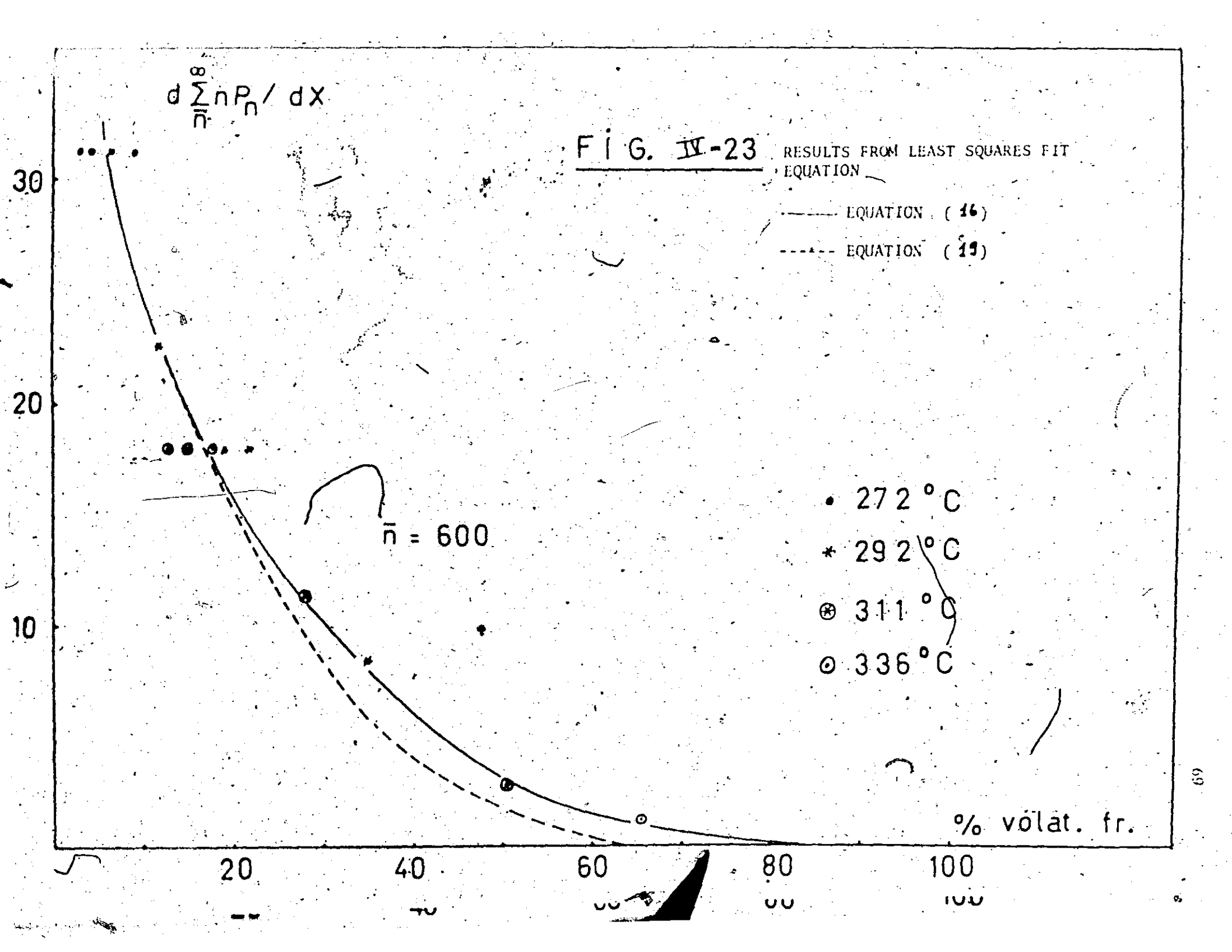
$d \sum_{\bar{n}}^{\infty} n P_n / dX$
FIG. IV-23
RESULTS FROM LEAST SQUARES FIT EQUATION
EQUATION (16)
EQUATION (19)
$\bar{n}$ = 600
• 272 °C
* 292 °C
⊛ 311 °C
⊙ 336 °C
% volat. fr.
30
20
10
20
40
60
80
100

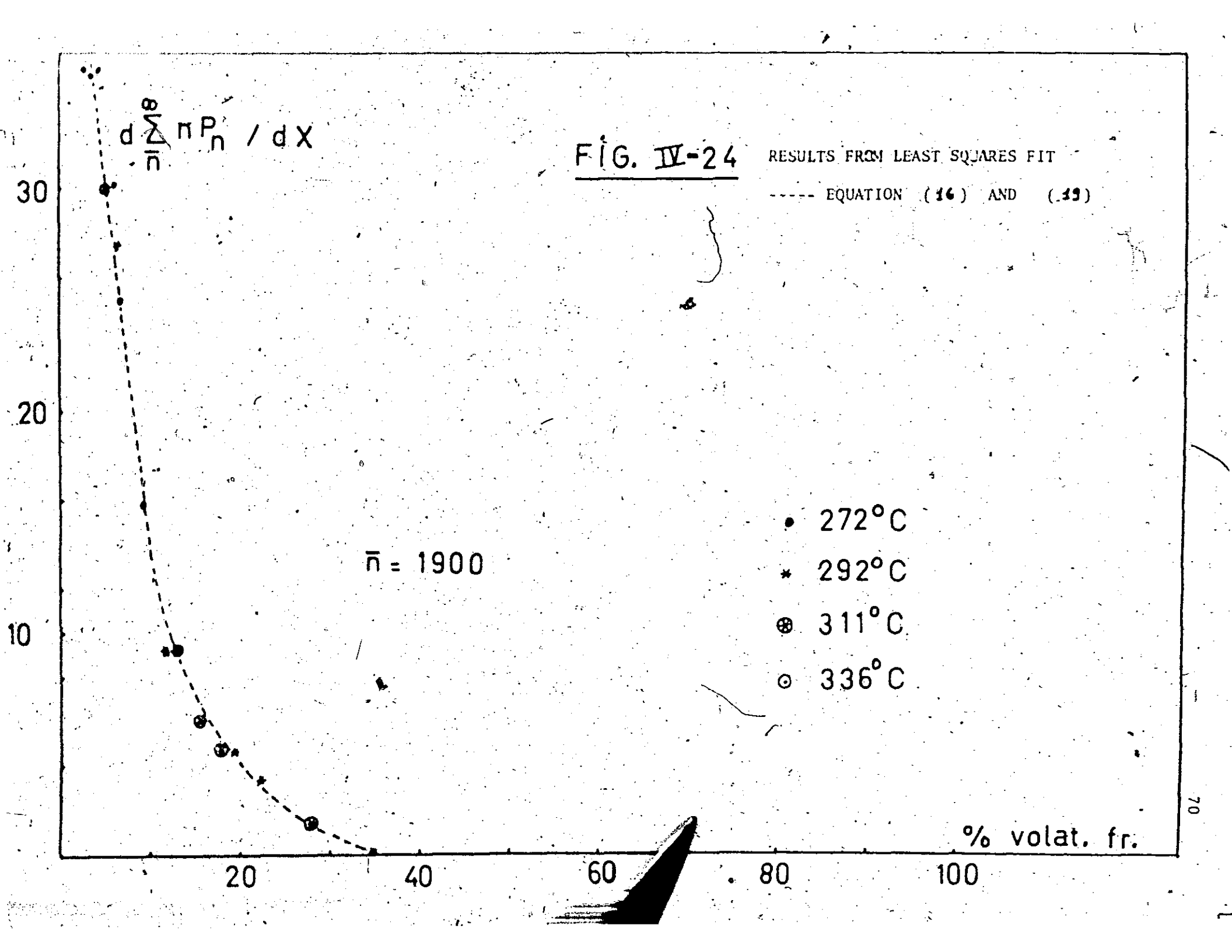

FIG. IV-24 RESULTS FROM LEAST SQUARES FIT

----- EQUATION (16) AND (19)

This was also confirmed by Cameron and Kerr [18], who, from the comparison of the rates of chain scission of two polymers which were both polymerized at 60°C, showed the rate of bond scission to exhibit a direct dependence on the initial molecular weight:

polymer	$k^* \times 10^5$ (hr^{-1})	$\bar{M}n_o \times 10^{-6}$
$TPS_{/2}$	5.86	1.490
$TPS_{/3}$	1.48	1.044

*see IV-6: Introduction to scission

The scission constants we obtained up to now however must be kind of average for all the chains larger than $\bar{n}$. A chain length dependence can however be extracted if we remark that for this polymer the average chain length

$$\frac{\sum_{n=\bar{n}}^{\infty} n P_n}{\sum_{n=\bar{n}}^{\infty} P_n} \qquad \text{for} \quad \bar{n} > 1{,}900$$

stays almost constant (within 10%) during the period of degradation considered (up to 52% volatilization), before decreasing steeply before disappearance. This statement becomes clearer after a look at the GPC response curve: these molecular weights are situated at the tail of the response curve. So at 311°C the following scission constants could be obtained:

TABLE IV-8

$\bar{n}^p$	$n_{average}$	k_s (sec^{-1})
1,900	2,600	.3621 x 10^{-4}
2,900	3,700	.4892 x 10^{-4}
4,400	5,000	.6040 x 10^{-4}

Plotted in a double logarithmic diagram (figure IV-23) a linear dependence between k_s and molecular weight is found:

$$\log k_s = -2.188 - 0.76 \log M.W.$$

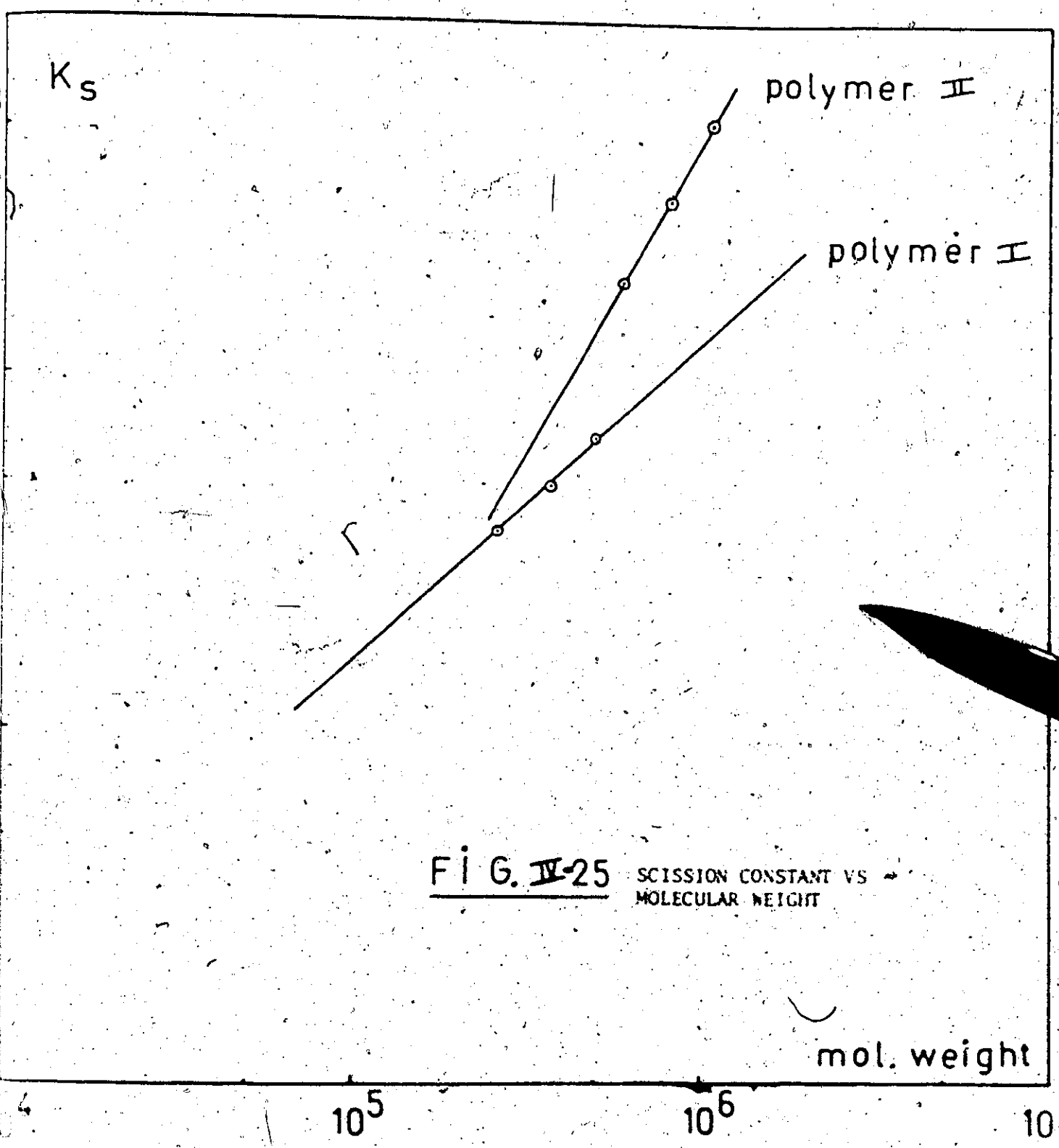

FIG. IV-25 SCISSION CONSTANT VS MOLECULAR WEIGHT

IV-9 Test of model 4

To test the validity of relation (20), between k_s and molecular weight, for other polymer samples, degassed styrenemonomer was thermally polymerized under 10^{-6} mm Hg vacuum at 111°C. The characteristics of this polymer (called polymer II) can be compared with the previous (polymer I) under table 1 in appendix 3. Polymer II was degraded at 311°C for up to 30 hours. The degradation path can be found back on the different figures as a dashed line. Using equation (17) and in a similar way as for polymer I, the k_s (n) for polymer II were obtained:

TABLE IV - 9

$\bar{n}$	$n_{average}$	k_s (sec^{-1})
4,400	6,000	$.1854 \times 10^{-3}$
6,400	8,200	$.3137 \times 10^{-3}$
9,300	11,000	$.5201 \times 10^{-3}$

The relation between k_s and molecular weight was now found to be

$$\log k_s = -31.25 + 1.703 \log M.W. \qquad (21)$$

From figure IV-25, where both relations (20) and (21) are plotted can be seen that the scission constants for the long chains of polymer II are much higher than could be forecasted from polymer I. This is also clear from figure IV-26: the decrease in polymer mass for polymer II

FIG. IV-26 POLYMER MASS, ONLY CONSIDERING CHAINS OF MORE THAN1900 UNITS, VS TIME AT DIFFERENT TEMPERATURES OF DEGRADATION

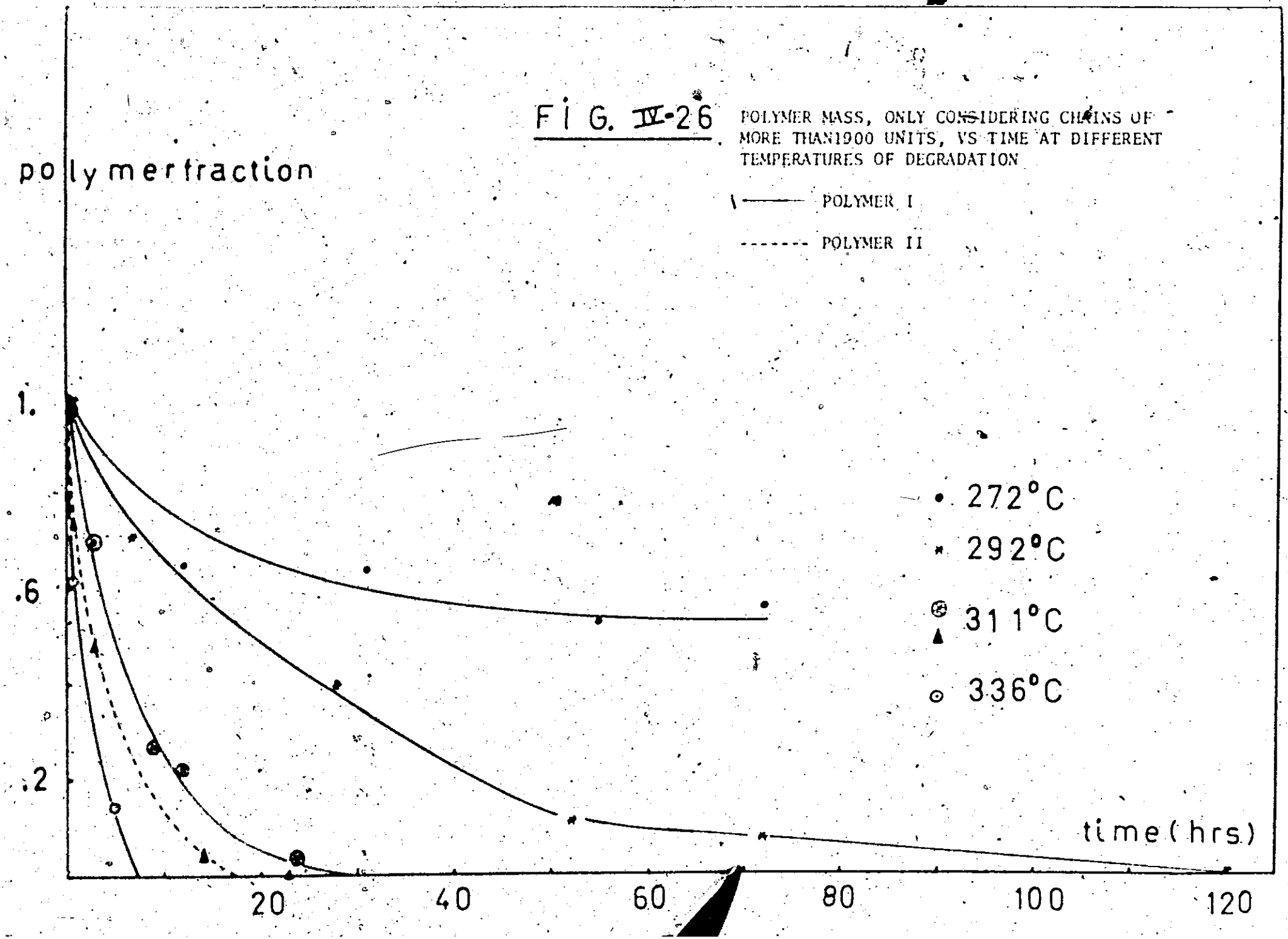

is at any moment faster than for polymer I.

At 311°C the rates of volatilization for both polymers as obtained from figure IV-1, are

polymer	rate of volatilization
I	2.72×10^{-6}
II	4.17×10^{-6}

Polymer II degrades faster than polymer I. The same conclusion is valid from the molecular weight curves, figure IV-4 and figure IV-5: the fall in average molecular weights is much greater for polymer II. Superposition was tried but no conclusions could be made.

Clearly the same Arrhenius plot as was used for polymer I, will not apply for polymer II.

V CONCLUSIONS AND RECOMMENDATIONS

Uninhibited styrene, degassed under high vacuum (10^{-6} mm Hg), was thermally polymerized in bulk at 10^{-6} mm Hg up to almost complete conversion. The samples so obtained were thermally degraded under the same high vacuum conditions at temperatures ranging between 270°C and 340°C. for different time intervals over the whole range of degradation. The breakdown of the polymer, through changes in number, weight average molecular weights, polydispersity, and molecular weight distribution, was investigated using gel permeation chromatography. The simple unzipping-mechanism from which we started was found to be inadequate in describing all experimental observations. Different other models were tried, from which finally a combination of random scission and depolymerization satisfied data best. The scission constants were determined and found to be functions of chain length.

To test this model polystyrene, prepared with the same careful exclusion of oxygen, but with completely different characteristics (e.g. polymerized at 111°C) was degraded at 311°C. The model was found to be applicable, but with completely different rate constants. This supposes the mechanism to be too simple and an additional step, relating different molecular weight distributions, to be included.

Although here the literature can provide a lot of new ideas not many are too useful. The most important were treated here.

Wall and coworkers [7] described their experimental observations on the thermal degradation of narrow distributed polystyrene by the results of computer calculations based on a mechanism involving initiation,

depropagation, intermolecular transfer, and transfer by disproportionation. The fit with the experimental data is not good at all, surely not at higher molecular weights. They attribute this to the occurrence of termination by combination and diffusion controlled rates.

Atkinson and MacCallum [19, 20] developed rate equations for the thermal decomposition of a polymer by a random scission reaction followed by rapid depolymerization of a constant number of monomer units from both fragments, together with rapid evaporation of low molecular weight species. Their theoretical curves could describe the weight loss and molecular weights as obtained from dynamic thermogravimetric analysis. However, no experimental data are given.

The largest difficulty is that up to now nobody really knows which steps govern the thermal degradation of polystyrene. So refers Cameron [21] to inter- and intra - molecular chain transfer as opposed to scission and depolymerization respectively.

The best agreement with experimental data was obtained by Gordon [22]. His model involved initiation, chain-end unzipping, intermolecular transfer and termination. However depending upon the initial molecular weight the order of the termination reaction had to be adapted, second-order for low molecular weight (230,000), and first order for high molecular weight (2,000,000) polystyrene. At intermediate molecular weights no fit could be obtained.

This leaves open the same question as in our mechanism: which step can relate the different molecular weight distributions? Gordon was also able through his model to explain the superposition of the mol-

ecular weight curves by assuming the activation energies for transfer and unzipping to be equal. This was found by us to be so.

The next step in the study of the thermal behavior of polystyrene should be the degradation of polymer samples with different initial molecular weight distributions, e.g. polymerized at different temperatures. This should give a clearer picture of the missing step in the mechanism which relates the behavior of different molecular weight distributions.

Although in the literature sophisticated models are described, the true model cannot be too complicated: the molecular weight curves superimpose, nice linear relationships are obtained etc.

VI REFERENCES

(1) L. A. Wall in G. M. Kline, ed., Analytical Chemistry of Polymers, Part II, Interscience Publishers, a division of John Wiley & Sons Inc., New York, 1962, p. 220 ff.

(2) S. L. Madorsky - Thermal Degradation of Organic Polymers, Interscience Publishers, a division of John Wiley & Sons, Inc., New York, 1964, pp. 26-91.

(3) Jellinek, J. Polymer Science, 3, 850 (1948); 4, 1, 13 (1949)

(4) N. Grassie and W. W. Kerr, Trans. Faraday Society, 55, 1050 (1959).

(5) N. Grassie and W. W. Kerr, Mackromol. Chemie, 51, 130 (1962).

(6) S. L. Madorsky, D. McIntyre, H. O'Mara, and S. Straus, J. Research Natl. Bur. Std., 66A, 307 (1962).

(7) L. A. Wall, S. Straus, J. H. Flynn, D. McIntyre and R. H. Simha, J. Phys. Chem., 70, 53 (1966).

(8) D. H. Richards and D. A. Salter, Polymer, 8, 153 (1967).

(9) G. G. Cameron and G. P. Kerr, European Polymer Journal, 1968, 4, 709 (1968).

(10) L. Reich, S. S. Stivala, "Elements of Polymer Degradation", McGraw-Hill Book Company (1971).

(11) R. H. Boundy and R. F. Boyer, "Styrene, its Polymers, Copolymers and Derivatives", Reinhold, p. 57

(12) A. N. Hui, Ph. D. thesis, Dept. of Chem. Eng., McMaster University (1970).

(13) T. Ishige, Ph. D. thesis, Dept. of Chem. Eng., McMaster University (1972).

(14) K. E. Coulton, H. Kehde, "Encyclopedia of Polymer Science and Technology", 1970, vol. 13, p. 136.

(15) F. W. Billmeyer, "Textbook of Polymer Science", Wiley-Interscience, 1971, pp. 369-372.

(16) D. Margerison, D. R. Bain and B. Kiely, "J. of Applied Polymer Science, March (1973).

(17) Odian, "Principles of Polymerization", McGraw-Hill (1970), p. 354.

(18) G. G. Cameron and G. P. Kerr, European Polymer J., 6, 423 (1970).

(19) J. Atkinson and J. R. MacCallum, J. Polym. Science A.2, Polymer Physics, 10, No. 5, 811 (1972).

(20) J. R. MacCallum, Europ. Polym. J., 7, 1237 (1971)

(21) G. G. Cameron, Europ. Polym. J., 6, 1601 (1970).

(22) M. Gordon, Trans. Faraday Society, 53, p. 1662 (1957).

APPENDIX

1. calculation of total number of polymer particles from the GPC response

The conversion from GPC chromatogram F(v)* to molecular weight fraction P(M) can be obtained as follows

$$F(v)\,dv = -F(M)\,dM \qquad (1)$$

or $$F(M) = -F(v)/(dM/dv)$$

The number of polymer molecules of molecular weight M, can be found as

$$P(M)\,dM = \frac{F(M)\,dM}{M}$$

The total number of molecules is then:

$$\int_0^\infty P(M)\,dM = \int_0^\infty \frac{F(M)\,dM}{M}$$

or in G.P.C. response terms and equation (1):

$$\int_{V_1}^{V_2} \frac{F(v)\,dv}{M(v)}$$

The so obtained number is the total number of grammoles of polymer of chain length n per gram of polymer. In order to convert this to gram-moles per liter of reacting mixture we have to multiply by:

$$(1-x)\,[\,\rho_m \cdot x - \rho_p\,(1-x)\,]$$

where x = % low molecular weight fraction

ρ_m = density of the monomer = 924 - 0.918 (T-273.1) g/l

ρ_p = density of the polymer* = 1084.8 - 0.605 (T-273.1) g/l

* from W. Patnode and W. J. Schëiber, J. Am. Chem. Soc., 61, 3449 (1939)

2. Second method for calculating the chain length dependence of the depropagation constant in model 2

This method is not as accurate as the first method. It gives the depropagation constant for a narrow range of molecular weights, where the constant is considered to be the same for the different chain lengths within the range.

Starting from the basic equation

$$\frac{dPn}{dt} = k_{dp}(n) \quad (P_{n+1} - P_n) \qquad (1)$$

Summation of equation (1) over a narrow molecular weight range, between chain length α and β gives

$$\frac{d \sum_{n=\alpha}^{n=\beta} P_n}{dt} = k_{dp_{\alpha,\beta}} \left(\sum_{n=\alpha}^{\beta} P_{n+1} - \sum_{n=\alpha}^{\beta} P_n \right)$$

Working out the summation, we get

$$\frac{d \sum_{n=\alpha}^{\beta} P_n}{dt} = k_{dp_{\alpha,\beta}} (P_{\beta+1} - P_\alpha) \qquad (2)$$

Left and right hand side of equation (2) should have the same sign at any time. This was found to be so.

As stated above the first method was preferred, since it gives k_{dp} corresponding to a specific chain length.

3. Tables

Table 1: Properties of the undegraded polymer samples

Characteristic	Units	Polymer I	Polymer II
Polymerization temperature	°C	168	111
Polymerization time	hour	40	60
Conversion	%	97	95
Mass of polymer	g/liter mixture	9.9	9.7
Number-average molecular weight		64,867	226,603
Weight-average molecular weight		168,453	518,000
Z-average molecular weight		282,746	753,034
Polydispersity		2.597	2.286
Total number of polymer particles	moles/ liter mixture	$.1652 \times 10^{-1}$	$.4666 \times 10^{-2}$

Table 2: $k_{dp}(\bar{n})$ at different temperatures

$\bar{n}$	k_{dp} (sec^{-1})			
	270	292	311	336
600	*	*	$.7205 \times 10^{-4}$	$.2476 \times 10^{-4}$
950	$.9197 \times 10^{-5}$	$.3355 \times 10^{-4}$	$.9287 \times 10^{-4}$	$.3209 \times 10^{-3}$
1,400	$.1111 \times 10^{-4}$	$.3777 \times 10^{-4}$	$.1123 \times 10^{-3}$	$.3656 \times 10^{-3}$
1,900	$.1345 \times 10^{-4}$	$.4455 \times 10^{-4}$	$.1256 \times 10^{-3}$	$.4712 \times 10^{-3}$
2,900	$.1521 \times 10^{-4}$	$.5457 \times 10^{-4}$	$.1525 \times 10^{-3}$	$.6799 \times 10^{-3}$

* k_{dp} ($\bar{n}$ = 600) for 270 and 292°C were not consistent anymore. From the graph of the total number of particles versus time still a slight rise could be seen.

Table 3: Degradation of polymer I at 270°C

Time (hours)	Volatile Fraction* %	Polymer Fraction** %	$\bar{M}_n$	$\bar{M}_w$	P.D.	Total Number*** of Polymer particles moles/liter mixture
0	2.94	100	62,567	156,197	2.496	$.1652 \times 10^{-1}$
0.	4.40	98.49	59,665	153,475	2.572	$.1702 \times 10^{-1}$
12	4.84	98.04	56,450	131,758	2.334	$.1789 \times 10^{-1}$
31	6.09	96.75	52,177	129,943	2.490	$.1907 \times 10^{-1}$
55	7.02	95.79	51,089	121,849	2.385	$.1925 \times 10^{-1}$
78	9.26	93.49	51,390	126,055	2.453	$.1861 \times 10^{-1}$

*Volatile fraction $= \dfrac{M}{M_o + (\sum n P_n)_n}$ where M includes monomer, dimer...pentomer

**Polymer fraction $= \sum_{n=2}^{\infty} n P_n \,/\, (\sum_{n=2}^{\infty} n P_n)_o$

***Total number of polymer particles $= \sum_{n=2}^{\infty} P_n$

Table 4: Degradation of polymer I at 292°C

Time (Hours)	Volatile Fraction %	Polymer Fraction** %	$\bar{M}_n$	$\bar{M}_w$	P.D.	Total Number of *** Polymer particles moles/liter mixture
0	3.03	100.	64,867	168,453	2.597	$.1591 \times 10^{-1}$
1	3.73	99.18	65,195	168,338	2.582	$.1570 \times 10^{-1}$
7	6.45	96.38	56,297	139,907	2.485	$.1759 \times 10^{-1}$
28	11.87	90.80	45,143	108,641	2.407	$.2089 \times 10^{-1}$
52	19.30	83.14	33,328	70,715	2.122	$.2593 \times 10^{-1}$
72	22.96	79.37	29,092	62,590	2.151	$.2729 \times 10^{-1}$
120	35.00	66.96	22,652	41,836	1.847	$.2899 \times 10^{-1}$

* Volatile Fraction $= \dfrac{M}{M_o + (\sum_{n=2}^{\infty} n P_n)_o}$ where M includes monomer, dimer...pentomer

**Polymer Fraction $= \sum_{n=2}^{\infty} n P_n \; / \; (\sum_{n=2}^{\infty} n P_n)_o$

***Total Number of Particles $= \sum_{n=2}^{\infty} P_n$

Table 5: Degradation of polymer I at 311°C

Time (Hours)	Volatile Fraction * %	Polymer Fraction ** %	$\bar{M}_n$	$\bar{M}_w$	P.D.	Total Number of *** Polymer particles moles/liter mixture
1	3.91	98.99	62,081	162,649	2.620	$.1645 \times 10^{-1}$
3	5.75	97.10	54,417	137,767	2.332	$.1836 \times 10^{-1}$
9	12.91	89.73	39,388	92,294	2.343	$.2317 \times 10^{-1}$
12	15.31	87.25	36,555	86,391	2.363	$.2418 \times 10^{-1}$
24	28.18	73.99	24,278	51,970	2.141	$.3024 \times 10^{-1}$
48	50.48	51.02	14,280	25,742	1.803	$.3414 \times 10^{-1}$
72	61.24	39.93	13,179	21,531	1.643	$.2842 \times 10^{-1}$

*Volatile Fraction $= \dfrac{M}{M_o + \left(\sum n P_n\right)_o}$ where M includes monomer, dimer...pentomer

**Polymer fraction $= \sum_{n=2} n P_n \Big/ \left(\sum_{n=2} n P_n\right)_o$

***Total number of polymer particles $= \sum_{n=2} P_n$

Table 6: Degradation of polymer I at 336°C

Time (hours)	Volatile* Fraction %	Polymer** fraction %	$\bar{M}_n$	$\bar{M}_w$	P.D.	Total Number of*** Polymer particles moles/liter mixture
1	5.87	96.97	50,329	130,445	2.592	$.1982 \times 10^{-1}$
5	18.00	84.48	33,130	75,437	2.277	$.2572 \times 10^{-1}$
21	65.50	35.54	10,306	16,952	1.645	$.3211 \times 10^{-1}$
44	87.50	12.88	7,604	10,566	1.390	$.1516 \times 10^{-1}$
68	98.70	1.34	7,409	8,195	1.106	$.1585 \times 10^{-2}$

*Volatile fraction = $\dfrac{M}{M_o + \left(\sum_{n=2}^{\infty} n P_n\right)_o}$ where M includes monomer, dimer...pentomer

**Polymer fraction = $\sum_{n=2}^{\infty} n P_n \Big/ \left(\sum_{n=2}^{\infty} n P_n\right)_o$

***Total Number of Particles = $\sum_{n=2}^{\infty} P_n$

Table 7: Degradation of polymer II at 311°C

Time (hours)	Volatile Fraction * %	Polymer Fraction ** %	Number-average molecular weight	Weight-average molecular weight	Poly-dispersity	Total number of polymer particles moles/liter mixture ***
0	5.42	100	226,603	518,000	2.286	$.4666 \times 10^{-2}$
1	7.82	97.5	116,947	315,261	2.696	$.8978 \times 10^{-2}$
5	10.3	94.8	85,055	212,295	2.496	$.1224 \times 10^{-1}$
14	29.35	74.7	28,906	58,190	2,013	$.3225 \times 10^{-1}$
23	38.80	64.7	23,406	43,302	1.850	$.3645 \times 10^{-1}$
29-1/2	48.25	54.7	20,334	32,708	1.609	$.3739 \times 10^{-1}$

*Volatile Fraction $= \dfrac{M}{M_o + \left(\sum_{n=2} n P_n\right)_o}$ where M includes monomer, dimer...pentomer

**Polymer Fraction $= \sum_{n=2} n P_n \Big/ \left(\sum_{n=2} n P_n\right)_o$

***Total Number of Particles $= \sum_{n=2} P_n$